AD-A053 734 VON KARMAN INST FOR FLUID DYNAMICS RHODE-SAINT-GENESE--ETC F/G 20/4
EXPERIMENTAL STUDY OF THE HYPERSONIC FLOW OVER CONVEX CONIC MOD--ETC(U)
1978 B E RICHARDS AFOSR-76-2942
UNCLASSIFIED VKI-IN-59 AFOSR-TR-78-0854 NL

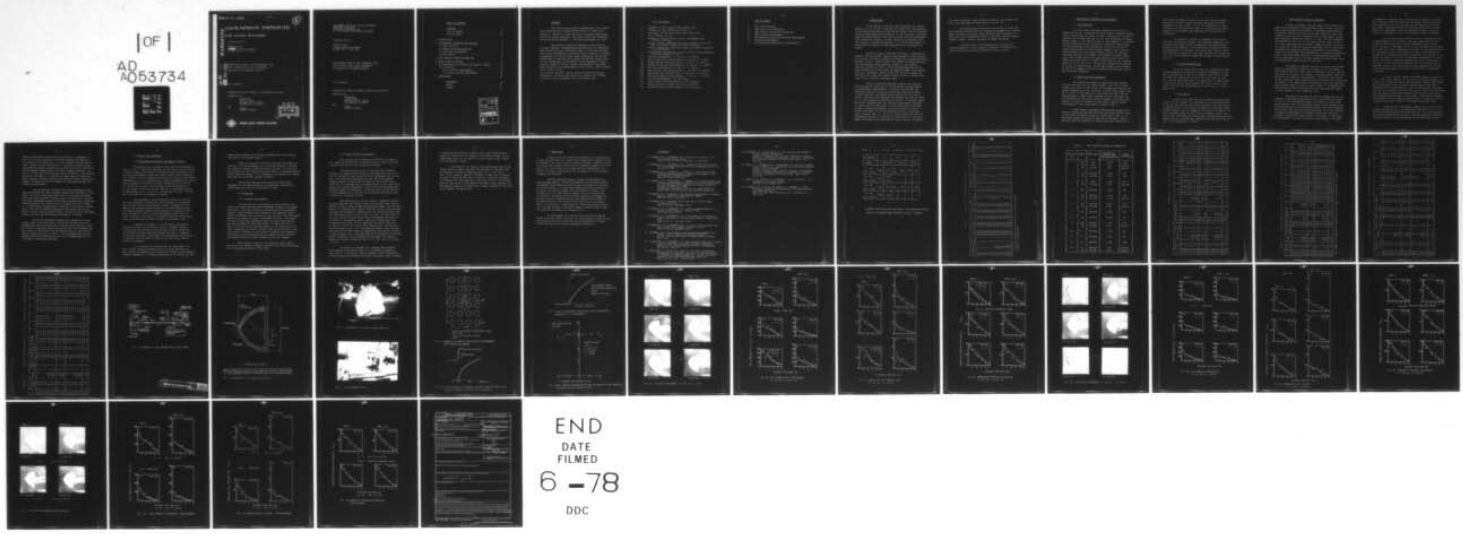

END
DATE FILMED
6 -78
DDC

(2)

von KARMAN INSTITUTE

FOR FLUID DYNAMICS

INTERNAL NOTE 59

AFOSR 76-2942

~~INTERIM~~ FINAL SCIENTIFIC REPORT
30 NOV 1976 - 1 DEC 1977

EXPERIMENTAL STUDY OF THE HYPERSONIC FLOW OVER A CONVEX CONIC MODEL RESEMBLING THE NOSETIP OF A REENTRY VEHICLE

B.E. RICHARDS

PREPARED FOR :

SAMSO/RSSE
PO BOX 92960
WORLDWAY POSTAL CENTER
LOS ANGELES, CA 90009

AND

EOARD
LONDON, ENGLAND

RHODE SAINT GENESE BELGIUM

VON KARMAN INSTITUTE FOR FLUID DYNAMICS
AEROSPACE DEPARTMENT
CHAUSSEE DE WATERLOO, 72
B - 1640 RHODE SAINT GENESE, BELGIUM

INTERNAL NOTE 59

AFOSR 76-2942

INTERIM SCIENTIFIC REPORT
30 NOV 1976 - 1 DEC 1977

EXPERIMENTAL STUDY OF THE HYPERSONIC FLOW OVER A CONVEX CONIC MODEL RESEMBLING THE NOSETIP OF A REENTRY VEHICLE

B.E. RICHARDS

PREPARED FOR :

SAMSO/RSSE
PO BOX 92960
WORLDWAY POSTAL CENTER
LOS ANGELES, CA 90009

AND

EOARD
LONDON, ENGLAND

TABLE OF CONTENTS

FOREWORD i
LIST OF FIGURES ii
LIST OF TABLES iii

1. INTRODUCTION 1

2. EXPERIMENTAL APPARATUS AND PROCEDURE 3
   2.1 Test facility 3
   2.2 Models and instrumentation 3
   2.3 Schlieren photography 4
   2.4 Test matrix 4

3. HEAT TRANSFER SENSOR CALIBRATION 5

4. RESULTS AND DISCUSSION 8
   4.1 Presentation of results and general remarks . . . 8
   4.2 Discussion 9
      4.2.1 Pressure measurements 9
      4.2.2 Heat transfer measurements 10

5. CONCLUSIONS 12

REFERENCES 13
TABLES 15
FIGURES 23

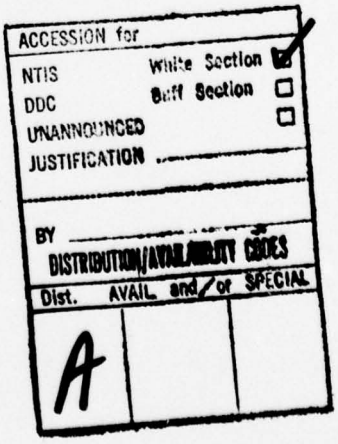

FOREWORD

The activities and results documented in this report were supported under Project 63311F with Lt E. Taylor and Captain R. Chambers of Space and Missile Systems Organization, acting as project engineers. The report covers work conducted during the period December 1, 1976 through November 30, 1977.

The technical advice and guidance by Mr Victor Di-Cristina, Manager, Thermodynamics and Materials Test Department, AVCO Systems Division, Wilmington, Mass., in the area of model design and instrumentation was particularly valuable. The author acknowledges the help of Mssrs Roger Conniasselle and Fernand Vandenbroek in operating the Longshot and Mr Jean-Claude Lobet for the photography. Mr Guy White, of the Department of Aeronautics, Imperial College, London, participated in the tests, data reduction and interpretation of the results, while carrying out a "stage" at VKI.
J-P Ville of VKI and D. Hardie and W.G. Borland of Paisley Polytechnic, Scotland, the latter also carrying out "stages" assisted in the development of the calibration rig.

LIST OF FIGURES

1 Schematic of the Longshot free piston tunnel

2 Schematic of the convex conic model K

3 Photograph of the rough convex conic model K(R)

4 CT1 calibrator set up

5 Geometry of array of holes used in impingement heat transfer calibrator

6 Typical surface temperature and heat transfer traces from thin film sensor subjected to CT1 calibrator

7 Typical temperature trace from copper calorimeter subjected to CT1 calibrator

8 Heat transfer distribution across an array of jets emanating from hole geometry of Fig. 5

9a Schlieren photographs, M = 16, Re = 9×10^6/ft

9b Heat transfer rate measurements, M = 16, Re = 9×10^6/ft

9c Normalized heat transfer rate, M = 16, Re = 9×10^6/ft

9d Normalized pressure measurements, M = 16, Re = 9×10^6/ft

10a Schlieren photographs, M = 20, Re = 3×10^6/ft

10b Heat transfer rate measurements, M = 20, Re = 3×10^6/ft

10c Normalized heat transfer rate, M = 20, Re = 3×10^6/ft

10d Normalized pressure measurements, M = 20, Re = 3×10^6/ft

11a Schlieren photographs, zero incidence

11b Heat transfer rate measurements, zero incidence

11c Normalized heat transfer rate, zero incidence

11d Normalized pressure measurements, zero incidence

LIST OF TABLES

1 Test identification
2 Test matrix and conditions
3 Heat sensor calibration information
4 Heat transfer measurements
5 Non-dimensionalized heat transfer measurements
6 Pressure measurements
7 Non-dimensionalized pressure measurements

1. INTRODUCTION

In the design of ablation type components for reentry vehicles, it is critical to be able to predict the flow behaviour on the complicated shapes evolved during flight. The full problem involves understanding the processes in, for instance, a boundary layer with mass addition from ablation with transition and maybe flow instability present. A useful input can be obtained from the testing of appropriate passive, i.e., non ablating models in flow conditions similar to that expected to be encountered in flight.

Because of lack of advanced facilities in operation at present, and for economic reasons, most parametric test programs are carried out at Mach numbers much below that encountered during the most critical reentry region with regard to maximum deceleration and maximum surface heating. Studies in the Longshot facility, described in Ref. 1, have the advantage that mainly exact simulation of Mach number and Reynolds number are achieved with full size models. Hence, using this facility, checks can be made on the lower Mach number studies as well as pinpointing other areas of further necessary study.

Studies to date include heat transfer and pressure distributions on simple 50°-8° biconic models and hemispheres. The experimental measurements in laminar, transitional and turbulent flow on a variety of smooth and rough walled models of this type with and without nose-bluntness and at various angles of attack, were compared with appropriate theories (Refs. 2 - 5). The studies on transition on the 50° - 8° biconic models were later extended (Ref. 6), pressure measurements were made on convex biconic shapes (Ref. 7) and studies were initiated on heat transfer measurements on concave biconic surfaces in steady flow (Refs. 9, 10) and unsteady pressures on concave conic surfaces (Ref. 11). In all of these studies the level of achievement has been in checking the feasibility of the measurement technique and to developing initial analyses to explain

the results obtained. Some further analyses of the results, however, have been made by DiCristina et al (Ref. 12).

The present series of tests, the results of which are here reported, concern the heat transfer measurements on a convex model representing another stable ablating shape and deals in particular with a methodical study of the effect of Mach number, Reynolds number, surface roughness and model incidence.

Included within is the description and results of the development of a heat transfer transducer calibration rig, useful to provide on-site verification of heat sensors.

2. EXPERIMENTAL APPARATUS AND PROCEDURE

2.1 Test facility

The von Karman Institute Longshot test facility as schematized in Fig. 1 was used for this program. Longshot differs from a conventional gun tunnel in that a heavy piston is used to compress the nitrogen test gas to very high pressures and temperatures (Refs. 1, 11). The test gas is then trapped in a reservoir at peak conditions by the closing of a system of check valves. The flow conditions decay monotically during 10 to 20 millisecond running times as the nitrogen trapped in the reservoir flows through the 6° half-angle conical nozzle into the pre-evacuated open jet test chamber. The extremes in supply conditions used in these tests are approximately 55,000 lb/in^2 at 1900°K and 38,000 lb/in^2 at 2320°K. These provide unit Reynolds numbers of 8.5×10^6 and 2×10^6 per ft at nominal Mach numbers of 15 and 20, respectively. The two Mach numbers were obtained at the 14 in diameter nozzle exit plane by using throat inserts with different diameters.

2.2 Models and instrumentation

The convex conic model is supplied by AVCO Systems Division and had a 0.25 in radius nosetip and a 6.25 in base diameter (see Fig. 2). The radius of the generator defining the convex forebody was 4.843 in giving a surface angle change from 64° to 11°45' to the model axis. The unmodified model was designated Model K. Model K(R) consisted of this same model but with the whole of the convex surface roughened by glueing metal spheres of 0.065 in diameter to the original smooth surface. A photograph of the latter model is shown in Fig. 3.

Twelve copper calorimeter heat transfer gauges manufactured by BBN and supplied with the models were mounted flush axially along the model surface as illustrated in Fig. 2. An additional gauge was placed on the nose of the model. Twelve pressure taps were identically spaced along the surface but at

180° around the model from the row of heat transfer gauges. Details of the heat sensors used and associated recording equipment is given in Refs. 3, 13. The calibration of these transducers is described in Chapter 3. Steady pressure measurements on these models were made using PCB piezoelectric transducers.

The reservoir pressure is measured using Kistler Type 6201 piezoelectric gauges. The reservoir temperature was assessed from signals from a tungsten-rhenium thermocouple mounted in the reservoir. Pitot pressures are measured with a PCB piezoelectric transducer. The tunnel test flow has undergone detailed calibration at the four standard test conditions using fine wire stagnation temperature probes as described in Ref. 14.

2.3 Schlieren photography

An 18 in conventional single pass Toepler schlieren system equipped with high quality optical components is used. With the exception of one 24 in diameter plane mirror to bend the light 90° (due to the vicinity of a wall near the test section) the light beam takes a Z-shaped path. A single spark light source with a spark duration of 1 μsec is used in all tests to record the visualization of the flow on 3¼ × 4¼ in sheet film.

2.4 Test matrix

Table 1 gives the scope of the test series and identifies the test number with each model and flow configuration. It can be seen that the test series provides cross sections of a complete matrix involving the parameters of flow Mach number, Reynolds number, surface roughness and angle of incidence. The test conditions given in this table are nominal values. The actual test conditions were calculated from appropriate measurements using the Longshot data reduction program (described in Ref. 3) and summarized in Table 2.

3. HEAT TRANSFER SENSOR CALIBRATION

Up until presently, the calorimeter heat sensors have been pre-calibrated by a oxy-acetylene flame or laser source by AEDC before mounting in the model. It has been recognized that an on-site calibration would be much more effective. Some experiments in the use of an isentropic light piston tunnel (a concept originally devised by Jones et al, Ref. 15) have suggested the adaptation of this facility to heat transfer sensor calibration. The experience so far gained in operating such a facility for studies of a turbine cooling system (Ref. 16) is that highly repeatable and steady performance at moderately high heating levels can be obtained. This performance is achieved economically with a relatively cheap facility and accompanying electronics and its adaptation to a calibrator seemed worth exploring. Tests so far made have used the VKI CT1 facility.

The method of applying the hot gas on the uncalibrated sensor was considered. Normally, in tests in CT1, the sensors are fitted flush with a test section side wall, the test section being used to simulate, for example, a passage between blades and end walls in a turbine. Disadvantages in using the same set up in the calibrator version would be lack of flexibility in mounting the sensors, and a poor usage of the heated flow since side wall heat transfer rates are low. A careful choice of streamwise position would also have to be made to ensure the gauge was always in fully laminar or fully turbulent flow.

The decision was made to directly impinge the test gas normally on the gauge flush mounted on a flat surface as shown in Fig. 4. This configuration would be expected to give higher heat transfer rates and furthermore gauges can be mounted easily as the heated gas can be allowed to exhaust into the laboratory and directly onto the sensor mounting plate. It is then required to choose an impingement configuration which will provide a spatially slow varying heat transfer distribution in the region of impingement, such that the lateral positioning of the gauge

is unimportant. Examples are a single hole or a matrix of smaller holes through which the heated gas can escape. Preliminary tests were made using thin film platinum surface temperature sensors and copper calorimeter sensors of the type used in the Longshot study, with impingement from gas escaping through an array of holes as illustrated in Fig. 5 and through a single 10 mm hole.

All the tests were carried out with a compression ratio of approximately 5 to 1 giving a test gas temperature of 470 K. A typical heat transfer and surface temperature trace for the thin film gauge is presented in Fig. 6. The analogue circuit used to process the surface temperature variation to give heat transfer was designed to give a rise time of 50 μsec, a running time of 50 msecs and a system sensitivity of about 65 μV per W/cm^2 (1 volt across the gauge, 2×10^{-3} per °K temperature coefficient of resistance). Except for a weak unsteadiness for the first 20 msecs, the trace is seen to be quite steady with a slight decay in heat transfer caused by the significant surface temperature rise. The trace was extrapolated to the start of the test to rationalize the results.

A trace from the copper calorimeter gauge is given in Fig. 7. The trace, however, is not linear as one would expect for a perfectly constructed device sensing a near constant heat transfer distribution (again not quite constant due to the rise in temperature of the calorimeter), since in approximately 100 msecs the slope has decreased by a half the initial value. This indicates that the gauge suffers from important heat losses at the calorimeter temperature achieved in these times. These sensors, however, are designed for the Longshot running time of 10 msecs, and Fig. 7 indicates that good linearity is obtained during this time.

Using the thin film gauge, surveys across the free jet ejected through the array of holes were made at 24.3, 34.3, 44.3 and 59.3 mm downstream of the plate and at 0 and 1.6 mm from the horizontal centerline of the array. The most favourable distribution was found at 59.3 mm downstream of the plate and 1.6 mm

above the horizontal centerline and the result is presented in Fig. 8. It can be seen that a flat heat transfer distribution at a level of 15.8 watts/cm^2 ± 2.5% is achieved over the central 8 mm. During 15 tests carried out in a period of about an hour, the operating pressure varied by only 0.02 kg/cm^2 from 4.93 kg/cm^2 and the ambient temperature of the model changed from 22°6 C to 23°2 C. At the same test condition nearly 40 watts/cm was achieved by placing the sensor at 10 mm from a single hole of 10 mm diameter, however, the heat transfer distribution varied rapidly with change in lateral position and hence this configuration was considered unsatisfactory.

The calibration rig having thus been developed, it was used to calibrate the heat transfer sensors before mounting in the model. The study proved more useful than at first was envisaged since the traces obtained showed up small idiosyncrasies in these individual hand-made products, which either enabled more favourable interpretation of the traces from the Longshot tests to be made or, if sufficiently unfavourable, rejection of the sensor. Furthermore, since the environment subjected to the sensor was not dissimilar to that in the Longshot tunnel, the few faultily fabricated sensors could be determined before mounting in the model.

During the subsequent Longshot test program to be described, some of the heat sensors failed and new ones had to be manufactured. Some old ones used in previous tests were also used. The record of the heat sensors used during this test program, with the values of calibration from the present tests or from earlier tests at AEDC, are given in Table 3. The new gauges were given a nominal calibration constant and will be calibrated when the CT1 calibrator is next made available.

4. RESULTS AND DISCUSSION

4.1 Presentation of results and general remarks

The overall basic results of the study are presented in Figs. 9, 10, 11. These are displayed in such a way as to facilitate the discussion of the effects of changing various parameters. The schlieren photographs, dimensional heat transfer rate, normalized heat transfer rate and normalized pressure are given in the figures designated a, b, c, d, respectively. Figure 9 represents the results taken on models K and K(R) at nominal conditions of M = 16 and Re = 9×10^6 per ft; Fig. 10 gives those on the same models at M = 20 and Re = 9×10^6 per ft. The final Fig. 11 presents results on these models at M = 16 and Re = 4.5×10^6 per ft, and M = 20 and Re = 2×10^6 per ft at zero angles of attack.

The experimental and normalized results for all tests are also presented in Tables 3-6. The pressures are normalized with respect to the pitot pressure, which is assumed to be the same as the stagnation point pressure. The heat transfer rates are normalized with respect to the theoretical stagnation point heat transfer on a 0.25 in radius hemisphere, whose value is given in Table 2, and which is calculated from free stream conditions using the Fay and Riddel formula as presented in Ref. 3.

A negative incidence, α, in the figures represents a "leeward" surface, and a positive value a "windward" surface. Since during one particular test, the heat transfer gauges are on a windward surface when the pressure taps are on a leeward surface and vice-versa, the figures are rearranged to align data on surfaces with the same attitude to the flow rather than in terms of run numbers.

It is pointed out also that for the rough model, the heat transfer gauges and pressure taps lie below the mean surface, and may be sensing local interactions caused by the roughness elements themselves. It is hence expected that the results on the

rough surfaces models will be more scattered and less accurate than those on the smooth models.

There is a distinct indication that the heat sensor at position 4 (at approximately 1.2 in from the nosetip) is giving low readings, despite calibration before the test. In the following discussion, the reading from this sensor is increased mentally by 30% above its reading. It is intended to recalibrate this sensor when next the calibrator becomes available.

The missing readings arose because of heat sensor breakages. At the time of testing no spares were available to replace them for that particular phase of test.

4.2 Discussion

4.2.1 Pressure measurements

The pressure data was checked for the purpose of the report with simply applied modified Newtonian theory, and tangent cone theory. Both these theories overpredicted the measurements, however, closer agreement was obtained by the Newtonian theory (which is compared with the data in Figs. 9d, 10d, 11d) even though tangent cone theory is usually considered realistic. The reason for this is that both theories neglect the centrifugal effects and the inaccuracy of the former theory is offset by this. A small error also arises from the neglect of the conicity of the flow in applying the theory. No other code for prediction of the flow field is available to the author at present for predicting the pressure distribution and the data awaits further analysis from codes available at AVCO Systems Division for example.

More scatter is seen in the rough wall data, mainly because of the roughness elements creating local flow interactions thus distorting the overall flow field.

4.2.2 Heat transfer measurements

Only qualitative examination of the data was made at this stage due to the lack of availability of a code for predicting the flow field at the Institute at present.

The most striking result is that the heat transfer rate due to roughening the surface is decreased over the first half of the body in most cases and fairly unchanged over the rear part. The schlieren photographs indicate that the roughness elements greatly increase the thickness of the initial shock layer and it is thought that this modification in the flow field causes this unusual phenomenon. It should also be mentioned that the heat sensors are generally lying below the average surface of the roughened wall, and will not be sensing the overall heat transfer to a roughened surface.

From experience in earlier studies, completely laminar flow was obtained over bodies, similar to the ones under test at present in the high Mach number low Reynolds number flow condition; hence it is expected that laminar flow will also be achieved under the same flow conditions. Comparison of the normalized heat transfer distribution plots given in Figs. 9c, 10c, 11c with those in Fig. 11c iii) and 11c iv) should give a reasonable indication of the state of the boundary layer. Taking the smooth model zero incidence cases first, such a comparison illustrates that the $M = 20$, $Re = 3\times10^6$ /ft is also fully laminar, but that the two low Mach number cases (i.e., high Reynolds number cases) undergo transition at an early stage as indicated by the overall increase in heat transfer rate. The rough model zero incidence distributions remain remarkably little affected by Mach number and Reynolds numbers as found by comparing Figs. 9c iv), 10c iv), 11c ii) and 11 c iv).

The effect of incidence on a laminar heat transfer distribution on the smooth model is illustrated by comparing Figs. 10c i), iii) and iv). Similar changes in heat transfer as in the pressure distributions are seen, such that a small increase

is obtained with positive incidence and a small decrease with negative incidence with no change in distribution shape. On the rough model (10c ii), iv) and vi)) little change in heat transfer distribution is seen.

The effect of incidence on the smooth model data at the higher Reynolds number case when the presence of turbulent flow is discerned is found by comparing Figs. 9c i), iii) and v). Very little change at negative incidence is seen, but a distinct increase in heat transfer rate is seen for a positive incidence of 3 degrees. For the rough wall case (Figs. 9c ii), iv) and iv)) there is seen to be a small general increase in heat transfer for the negative angle of incidence and a larger increase for the positive 3 degree incidence case.

5. CONCLUSIONS

Pressure and heat transfer measurements and visualization of the flow were made on a convex conic shape with a spherical nose-tip tested in the flow of the von Karman Institute Longshot facility at nominal Mach numbers of 16 and 20 and Reynolds numbers of 9.0×10^6 and 4.5×10^6, and 3.0×10^6 and 2.0×10^6 per ft, respectively. The effect of surface roughness and flow incidence of $\pm3°$ on the measurements was studied.

Modified Newtonian theory slightly overestimates the pressure measurements. From simple comparison of the heat transfer measurements with themselves and previous exoeriments carried out on similar bodies, it is concluded tentatively that the Mach 20, and hence low Reynolds number cases are generally laminar, and the Mach 15, i.e., high Reynolds number cases are transitional or turbulent. Roughness caused the heat transfer measurements to decrease, such an unexpected result was tentatively ascribed to the modification of the inviscid flow field, but also somewhat due to the difficulty in measuring (or interpreting) heat transfer data to rough surfaces. Only small changes in heat transfer rate are found due to changes of incidence of $\pm3°$.

The development of an onsite heat transfer calibrator proved to be most useful, not only for calibrating the supplied heat heat sensors, but also simplifying the interpretation of signal traces and selecting the best performing transducers.

REFERENCES

1. RICHARDS, B.E. & ENKENHUS, K.R.: Hypersonic testing in the VKI Longshot piston tunnel.
AIAA J., Vol. 8, No 6, June 1970, pp 1020-1025.

2. RICHARDS, B.E. & ENKENHUS, K.R.: Stagnation point heat transfer and pressure distribution on a hemipshere at M = 15.
VKI TR 39, 1970.

3. RICHARDS, B.E.; CULOTTA, S.; SLECHTEN, J.: Heat transfer and pressure distributions on reentry nose shapes in the VKI Longhsot hypersonic tunnel.
AFML TR 71-200, June 1971.

4. RICHARDS, B.E.; DiCRISTINA, V.,; MINGES, M.L.: Heat transfer and pressure distribution on sharp and finite bluntness biconic and hemispherical geometries at various angles of attack in a Mach 15-20 flow.
Astronautical Research 1971; ed. L.G. Napolitano; D. Reidel Publ. Co, Dordrecht, Holland 1973; pp 91-103.

5. RICHARDS, B.E.: Hypersonic heat transfer measurements on reentry vehicle surfaces at high Reynolds number.
AFML TR 73-187, June 1973.

6. RICHARDS, B.E.: Boundary layer transition on blunt bodies in hypersonic flow.
AFML TR 75-139, September 1975.

7. RICHARDS, B.E. & KENWORTHY, M.A.: Pressure measurements on a convex biconic model in a Mach 15 flow.
VKI TR 84, March 1974.

8. RICHARDS, B.E. & KENWORTHY, M.A.: The study of the effect of shock interaction on concave conic shapes in hypersonic flow.
AFML TR 75-137, September 1975.

9. KENWORTHY, M.A. & RICHARDS, B.E.: A study of the unsteady flow over concave conic model at Mach 15 and 20.
AFML TR 75-138, September 1975.

10. RICHARDS, B.E.: Heat transfer and pressure measurements on a concave biconic model with flattened nosetip.
VKI TR 58, Interim Scientific Report AFOSR 76-2942, March 1977.

11. DiCRISTINA, V. & RICHARDS, B.E.: Heat transfer studies on ablation protected nosetips at reentry simulated conditions.
AIAA P 77-781; 12th Thermophysics Conf., Albuquerque, New Mexico, June 1977.

12. DiCRISTINA, V.; CHEN, K.K.; LIN, T.; LIU, T.M.: Exploratory development of hypersonic heat transfer and thermochemical ablation of advanced materials: nosetip test data evaluation and rough wall transition analysis.
AFML TR 75-25, Vol. 1, April 1975.

13. RICHARDS, B.E.: Developments in heat transfer measurements using transient techniques.
ICIASF' 77 Record. Proc. 7th Int. Congress on Instrumentation in Aerospace Simulation Facilities; Shrivenham UK, IEEE Publication 77 CH 1251-8 AES, Sept. 1977, pp 81-88.

14. BACKX, E. & RICHARDS, B.E.: Measurement of stagnation temperatures of 2500 K in a hypersonic flow of 10 msec duration using a fine wire probe.
ICIASF'77 Record. Proc. 7th Int. Congress on Instrumentation in Aerospace Simulation Facilities; Shrivenham UK, IEEE Publication 77 CH 1251-8 AES, Sept. 1977, pp 95-100.

15. JONES, T.V.; SCHULTZ, D.L.; HENDLEY, A.D.: On the flow in an isentropic free piston tunnel.
ARC R&M 3731, January 1973.

16. RICHARDS, B.E.; VILLE, J-P; APPELS, C.; SALEMI, C.: Film cooling of heated turbine surfaces at representatively simulated conditions.
AIAA P 77-947, 13th Propulsion Conf., Orlando, Fla. July 1977.

TABLE 1 - TEST IDENTIFICATION

INCIDENCE	0°		+3°†		-3°	
MODEL	K	K(R)	K	K(R)	K	K(R)
M = 16※ Re = 9×10^6	566	575	573 574	582	572	583
M = 16※ Re = 5×10^6	567	576 577	-	-	-	-
M = 20※ Re = 3×10^6	568	579	570	581	571	580
M = 20※ Re = 2×10^6	569	578	-	-	-	-

※ nominal test conditions see Table 2 for measured values

† positive incidence means pressure surface "leeward"

TABLE 2 - TEST MATRIX AND CONDITIONS

RUN	MODEL	INCID. (deg.)	P_0 (lb/in^2)	$P_{0_{perf}}$ (lb/in^2)	T_0 (K)	$T_{0_{perf}}$ (K)	T_{stag} (K)	p_{t_2} (lb/in^2)	M	Re 10^{-6} (ft^{-1})	$p \times 10^2$ (lb/in^2)	T (K)	T_{cond} (K)	V (ft/sec)	$\frac{Q^+}{BT_h u}$ ($\frac{}{ft^2 sec}$)
566	K	0	52,900	75,900	1890	2420	2170	27.8	15.6	9.0	8.7	49	44	7290	360
567	K	0	36,000	41,300	2000	2460	2200	18.2	15.0	5.3	6.2	53	42	7340	295
568	K	0	54,900	63,200	2400	3070	2690	7.8	19.5	2.9	1.57	40	36	8240	251
569	K	0	43,200	43,600	2510	3130	2740	5.6	19.4	1.9	1.13	41	35	8320	216
570	K	+3	58,600	70,340	2370	3060	2680	8.2	19.7	3.1	1.48	37	36	8100	255
571	K	-3	60,200	72,950	2380	3080	2700	7.9	20.0	3.1	1.52	38	36	8250	253
572	K	-3	56,600	84,800	1870	2440	2180	26.0	16.2	9.1	7.6	46	43	7310	348
573	K	+3	55,850	83,000	1870	2430	2170	30.6	15.6	9.9	9.7	49	44	7300	377
574*	K	+3	56,700	84,200	1890	2460	2190	28.0	15.9	9.3	8.5	48	44	7340	365
575	K(R)	0	58,800	88,800	1890	2480	2210	29.4	15.9	9.7	8.9	48	44	7370	377
576	K(R)	0	33,290	37,400	1990	2420	2160	18.0	14.8	5.2	6.3	54	42	7280	287
577*	K(R)	0	33,100	36,800	2010	2440	2180	18.6	14.6	5.1	6.7	56	42	7310	295
578	K(R)	0	40,100	40,300	2450	3040	2670	5.4	19.2	1.9	1.13	41	35	8200	206
579	K(R)	0	55,800	65,300	2380	3050	2670	8.0	19.5	3.0	1.61	39	36	8200	252
580	K(R)	+3	58,500	69,400	2390	3090	2700	8.2	19.7	3.0	1.61	39	36	8260	257
581	K(R)	-3	57,400	68,100	2370	3050	2680	8.3	19.6	3.1	1.67	39	36	8210	257
582	K(R)	-3	54,200	80,600	840	2380	2130	26.1	16.0	9.2	7.82	46	43	7230	340
583	K(R)	+3	61,300	93,300	1920	2530	2250	30.0	16.0	9.6	9.0	48	44	7450	390

+ theoretical stagnation point heat transfer on 0.25 in radius hemisphere

* repeat runs of preceding test

TABLE 3 - HEAT SENSOR CALIBRATION INFORMATION

POSITION No	GAUGE	RUNS USED	CALIBRATION CONSTANT USED BT_h U/ft^{2}sec/mV/sec	WHERE CALIBRATED
1	12A	566	1.016	AEDC
	3B	575	1.00	uncalib.
	7B	577-583	1.00	uncalib.
2	8A	566-576	1.023	VKI
	5A	577-583	1.225	VKI
3	1A	566	0.762	VKI
	4B	575-583	1.00	uncalib.
4	13A	566-583	1.236	VKI
5	2A	566-576	1.119	VKI
	1B	577-583	1.000	uncalib.
6	5A	566-576	1.225	VKI
	6B	577-583	1.00	uncalib.
7	11A	566-583	0.800	VKI
8	9A	566-583	0.796	VKI
9	15A	566-576	1.179	VKI
	2B	577-583	1.00	uncalib.
10	13	566-583	1.315	VKI
11	15	566-583	1.355	VKI
12	18	566-583	1.682	AEDC
13	6	566-574	1.00	uncalib.
	8B	575-583	1.00	uncalib.

TABLE 4 - HEAT TRANSFER MEASUREMENTS

M	$Re \times 10^{-6}$ (ft^{-1})	MODEL	INCID. (deg.)	RUN No	STAG pt	GAUGE 2	3	4	5	6	7	8	9	10	11	12	13
15.6	9.0	K	0	566	-	217	-	179	210	151	137	132	103	56	45	37	3
15.6	9.9	K	+3	573	-	300	-	200	300	229	185	115	-	73	64	57	-
15.9	9.3	K	+3	574	-	351	-	181	261	210	168	133	122	84	76	61	-
16.2	9.1	K	-3	572	-	316	-	187	219	200	154	171	138	53	51	40	1
15.9	9.7	K(R)	0	575	-	142	115	85	107	78	77	54	36	29	21	17	11
16.0	9.2	K(R)	+3	582	453	108	156	133	117	160	120	81	60	46	32	27	3
16.0	9.6	K(R)	-3	583	558	189	189	161	122	170	133	64	67	43	37	11	-
15.0	5.3	K	0	567	-	220	-	109	140	142	118	105	94	50	45	26	3
14.8	5.2	K(R)	0	576	-	193	149	112	104	-	81	-	-	34	28	21	13
14.6	5.1	K(R)	0	577	388	124	120	94	75	79	80	45	25	23	24	16	2
19.5	2.9	K	0	568	-	189	-	87	94	84	70	52	37	24	26	14	2
19.7	3.1	K	+3	570	-	232	-	122	111	96	86	57	45	24	23	20	1
20.0	3.1	K	-3	571	-	209	-	94	88	84	72	56	41	19	19	12	1
19.5	3.0	K(R)	0	579	298	107	-	62	73	84	59	29	29	20	11	3	1
19.6	3.1	K(R)	+3	581	349	101	87	91	85	89	66	44	71	16	22	11	1
19.7	3.1	K(R)	-3	580	425	101	84.5	67	64	71	53	31	51	21	9	5	1
19.4	1.9	K	0	569	-	143	-	73	89	41	39	38	26	15	15	11	-
19.2	1.9	K(R)	0	578	345	99	61	46	38	54	39	26	20	12	8	2	1

TABLE 5 - NON-DIMENSIONALIZED* HEAT TRANSFER MEASUREMENTS

M	Re×10^{-6} (ft^{-1})	MODEL	INCID. (deg.)	RUN No	STAG pt	GAUGE 2	3	4	5	6	7	8	9	10	11	12	13
15.6	9.0	K	0	566	-	0.60	-	0.50	0.58	0.42	0.38	0.37	0.29	0.16	0.125	0.10	0.01
15.6	9.9	K	+3	573	-	0.80	-	0.54	0.80	0.61	0.50	0.31	-	0.20	0.17	0.15	-
15.9	9.3	K	+3	574	-	0.96	-	0.50	0.71	0.57	0.46	0.36	0.33	0.23	0.21	0.17	-
16.2	9.1	K	-3	572	-	0.91	-	0.54	0.63	0.57	0.44	0.49	0.40	0.15	0.15	0.12	0.003
15.9	9.7	K(R)	0	575	-	0.38	0.30	0.23	0.28	0.21	0.20	0.14	0.10	0.08	0.06	0.045	0.03
16.0	9.2	K(R)	+3	582	1.33	0.32	0.46	0.39	0.34	0.47	0.35	0.24	0.18	0.14	0.09	0.08	0.01
16.0	9.6	K(R)	-3	583	1.43	0.49	0.49	0.41	0.31	0.44	0.34	0.16	0.17	0.11	0.10	0.03	-
15.0	5.3	K	0	567	-	0.75	-	0.37	0.47	0.48	0.40	0.36	0.32	0.17	0.15	0.09	0.01
14.8	5.2	K(R)	0	576	-	0.67	0.52	0.39	0.36	-	0.28	-	-	0.12	0.10	0.07	0.05
14.6	5.1	K(R)	0	577	1.32	0.42	0.41	0.32	0.25	0.27	0.27	0.15	0.08	0.08	0.08	0.05	0.01
19.5	2.9	K	0	568	-	0.75	-	0.35	0.37	0.33	0.28	0.21	0.15	0.10	0.10	0.06	0.01
19.7	3.1	K	+3	570	-	0.91	-	0.48	0.43	0.38	0.34	0.22	0.18	0.09	0.09	0.08	0.004
20.0	3.1	K	-3	571	-	0.83	-	0.37	0.35	0.33	0.28	0.22	0.16	0.08	0.08	0.05	0.004
19.5	3.0	K(R)	0	579	1.18	0.43	-	0.25	0.29	0.33	0.23	0.12	0.12	0.08	0.04	0.01	0.004
19.6	3.1	K(R)	+3	581	1.36	0.39	0.34	0.35	0.33	0.35	0.26	0.17	0.28	0.06	0.09	0.04	0.004
19.7	3.1	K(R)	-3	580	1.65	0.39	0.33	0.26	0.25	0.28	0.21	0.12	0.20	0.08	0.04	0.02	0.004
19.4	1.9	K	0	569	-	0.66	-	0.34	0.43	0.19	0.18	0.18	0.12	0.07	0.07	0.05	-
19.2	1.9	K(R)	0	578	1.67	0.48	0.30	0.22	0.18	0.26	0.19	0.13	0.10	0.06	0.04	0.01	0.005

* With respect to the theoretical stagnation point heat transfer on 0.25 in sphere (see Table 2)

TABLE 6 - PRESSURE MEASUREMENTS (lb/in^2)

M	$Re \times 10^{-6}$ (ft^{-1})	MODEL	INCID. (deg.)	RUN No	PITOT PRESS.	GAUGE 2	3	4	5	6	7	9	11	13
15.6	9.0	K	0	566	27.8	20.4	18.5	16.8	13.9	9.8	8.9	5.7	3.0	1.4
16.2	9.1	K	+3	572	26.0	23.3	18.4	18.6	14.4	11.3	10.3	6.8	3.7	1.8
15.6	9.9	K	-3	573	30.6	20.9	19.2	15.9	13.7	11.2	8.1	5.2	2.6	1.1
15.9	9.3	K	-3	574	28.0	19.7	18.0	14.1	12.6	10.0	7.5	4.7	2.4	1.1
15.9	9.7	K(R)	0	575	29.4	20.0	18.3	14.2	14.5	11.3	8.8	6.0	4.5	1.7
16.0	9.6	K(R)	+3	583	30.0	22.5	18.5	18.0	-	12.4	9.3	6.9	4.1	2.3
16.0	9.2	K(R)	-3	582	26.1	17.1	16.3	15.8	-	10.7	6.6	4.5	2.3	1.3
15.0	5.3	K	0	567	18.2	14.3	11.6	11.2	9.2	6.5	5.3	3.5	1.9	0.9
14.8	5.2	K(R)	0	576	18.0	14.8	11.0	10.4	8.2	7.9	6.6	3.0	2.0	1.1
14.6	5.1	K(R)	0	577	18.6	14.9	12.5	9.9	9.3	7.8	6.0	3.5	2.0	1.2
19.5	2.9	K	0	568	7.8	6.7	5.8	5.0	3.9	3.0	2.5	1.6	0.9	0.5
20.0	3.1	K	+3	571	7.9	7.0	6.8	5.4	4.5	3.1	3.0	2.0	1.2	0.6
19.7	3.1	K	-3	570	8.2	6.2	5.7	4.4	3.7	3.1	2.2	1.5	0.8	0.4
19.5	3.0	K(R)	0	579	8.0	7.7	5.2	5.1	-	3.4	2.7	1.9	1.0	0.5
19.7	3.1	K(R)	+3	580	8.2	6.8	5.5	5.8	-	3.6	3.0	2.0	1.2	0.7
19.6	3.1	K(R)	-3	581	8.3	6.3	5.1	5.1	-	3.4	2.0	1.5	0.8	0.4
19.4	1.9	K	0	569	5.6	4.5	4.3	3.5	2.8	2.4	2.0	1.2	0.7	0.3
19.2	1.9	K(R)	0	578	5.4	4.6	4.2	3.4	2.5	2.3	-	1.2	0.6	0.3

TABLE 7 - NON-DIMENSIONALIZED PRESSURE MEASUREMENTS

M	$Re \times 10^{-6}$ (ft^{-1})	MODEL	INCID. (deg.)	RUN No	PITOT PRESS.	GAUGE 2	3	4	5	6	7	9	11	13
15.6	9.0	K	0	566	1.0	0.73	0.66	0.60	0.50	0.35	0.32	0.21	0.11	0.05
16.2	9.1	K	+3	572	1.0	0.89	0.70	0.72	0.55	0.44	0.39	0.26	0.14	0.07
15.6	9.9	K	-3	573	1.0	0.69	0.63	0.52	0.45	0.37	0.27	0.17	0.09	0.04
15.9	9.3	K	-3	574	1.0	0.70	0.64	0.51	0.45	0.36	0.27	0.17	0.09	0.04
15.9	9.7	K(R)	0	575	1.0	0.68	0.62	0.48	0.50	0.38	0.30	0.20	0.15	0.05
16.0	9.6	K(R)	+3	583	1.0	0.75	0.62	0.60	-	0.41	0.31	0.23	0.14	0.08
16.0	9.2	K(R)	-3	582	1.0	0.66	0.62	0.60	-	0.41	0.25	0.17	0.09	0.05
15.0	5.3	K	0	567	1.0	0.79	0.64	0.62	0.51	0.36	0.29	0.19	0.10	0.05
14.8	5.2	K(R)	0	576	1.0	0.83	0.61	0.57	0.46	0.44	0.37	0.17	0.11	0.06
14.6	5.1	K(R)	0	577	1.0	0.80	0.67	0.53	0.50	0.42	0.33	0.19	0.11	0.07
19.5	2.9	K	0	568	1.0	0.86	0.74	0.64	0.50	0.38	0.31	0.21	0.12	0.06
20.0	3.1	K	+3	571	1.0	0.89	0.85	0.68	0.56	0.39	0.37	0.25	0.15	0.07
19.7	3.1	K	-3	570	1.0	0.76	0.69	0.54	0.45	0.38	0.26	0.18	0.09	0.05
19.5	3.0	K(R)	0	579	1.0	0.96	0.66	0.74	-	0.43	0.35	0.24	0.13	0.07
19.7	3.1	K(R)	+3	580	1.0	0.83	0.67	0.71	-	0.45	0.37	0.25	0.14	0.08
19.6	3.1	K(R)	-3	581	1.0	0.76	0.62	0.62	-	0.41	0.24	0.18	0.09	0.05
19.4	1.9	K	0	569	1.0	0.82	0.79	0.62	0.50	0.42	0.36	0.22	0.13	0.06
19.2	1.9	K(R)	0	578	1.0	0.84	0.79	0.63	0.46	0.43	-	0.23	0.12	0.06

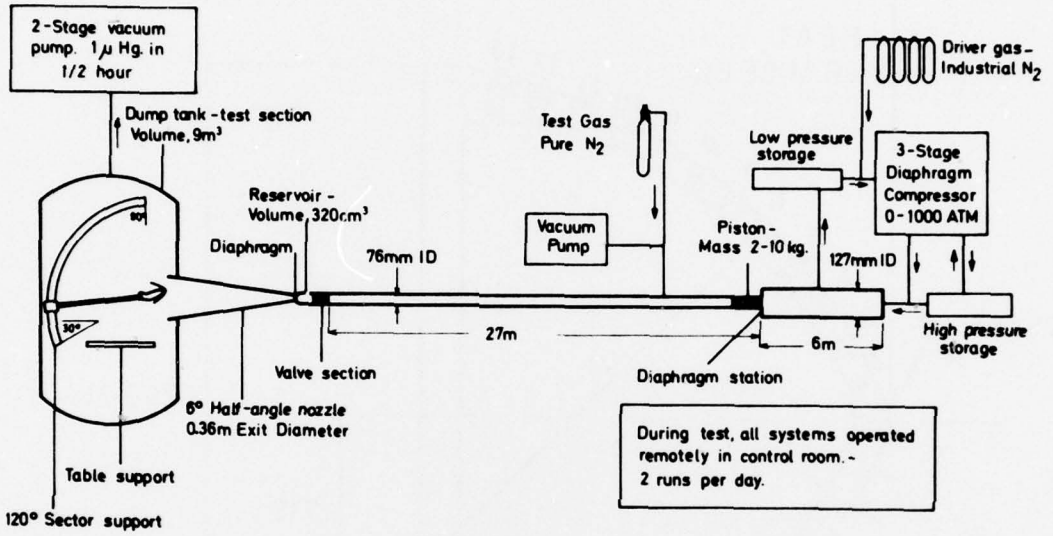

FIG. 1 SCHEMATIC OF THE LONGSHOT FREE PISTON TUNNEL

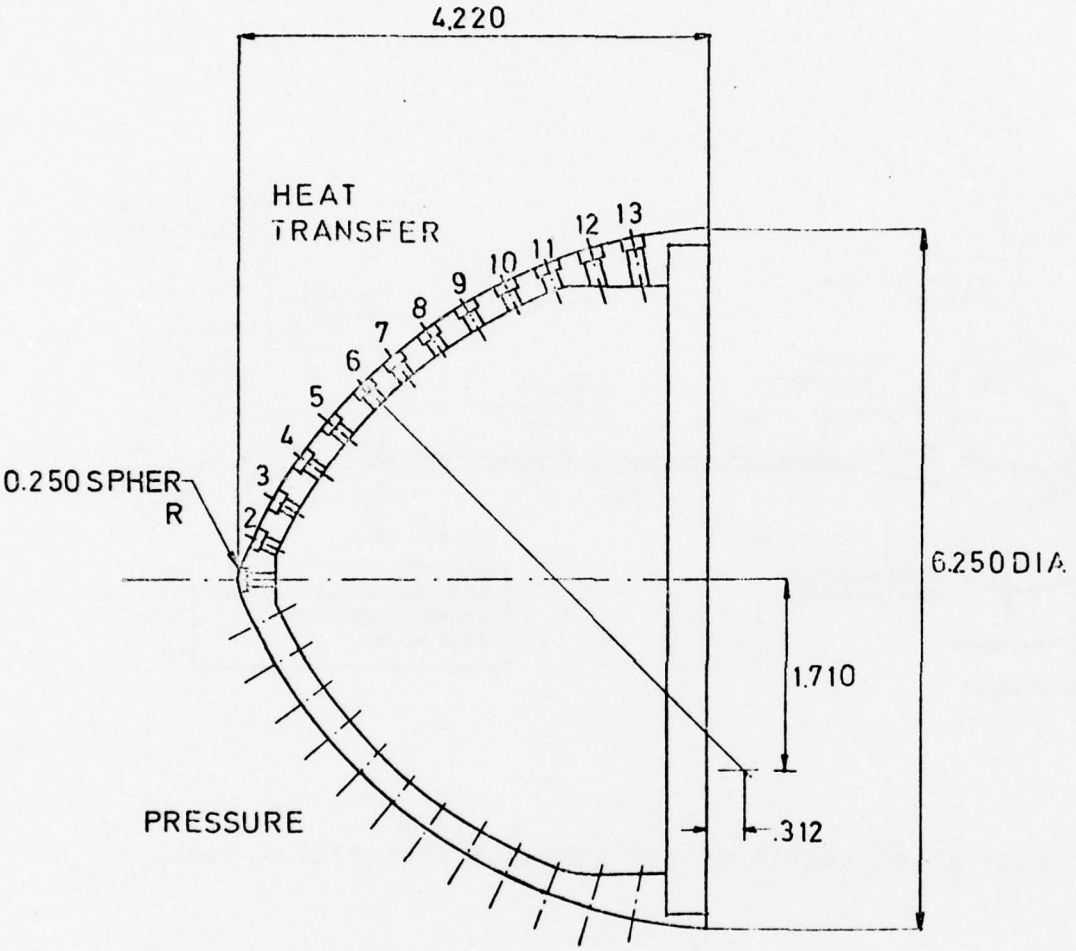

DIMENSIONS IN INCHES.

Pos.	2	3	4	5	6	7	8	9	10	11	12	13
	64	5925	54.5	4975	45	4025	35.5	3075	26	21.25	16.5	1175

FIG. 2 SCHEMATIC OF THE CONVEX CONIC MODEL K.

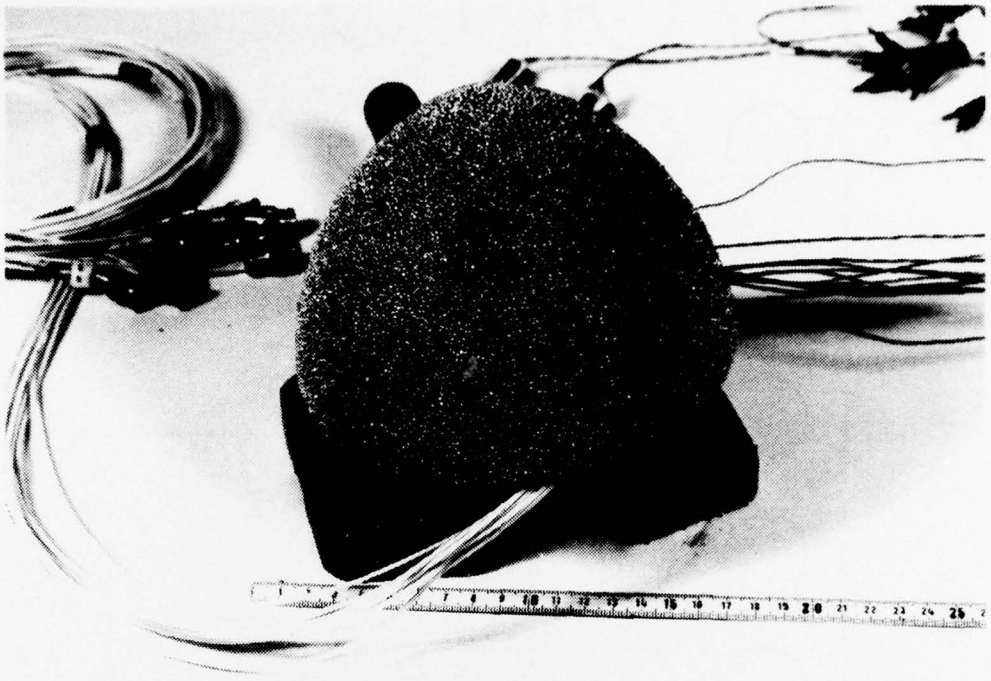

FIG. 3 PHOTOGRAPH OF THE ROUGH CONVEX MODEL K(R)

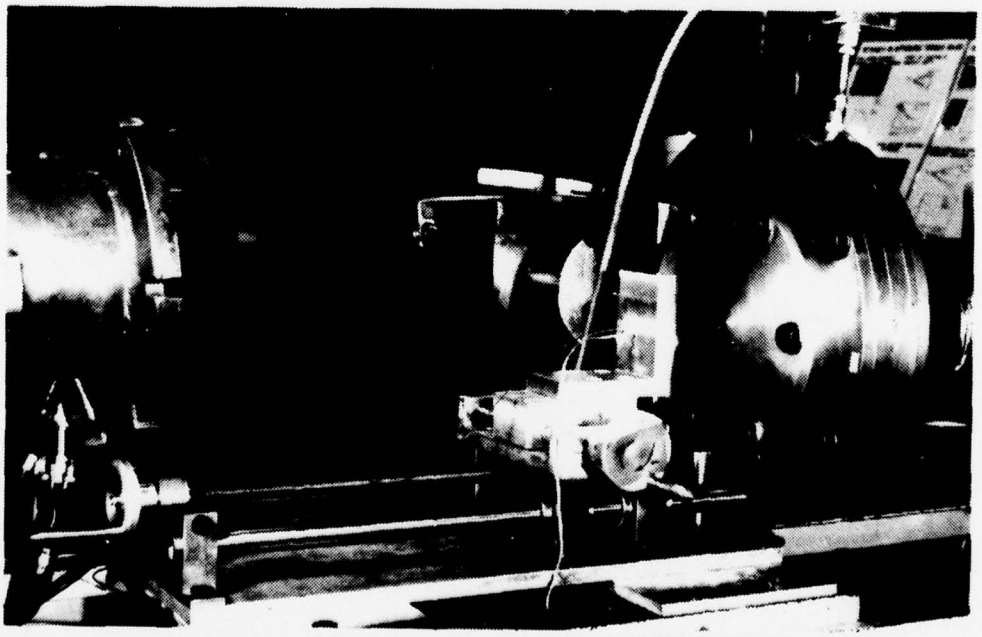

FIG. 4 CTI CALIBRATOR SET UP

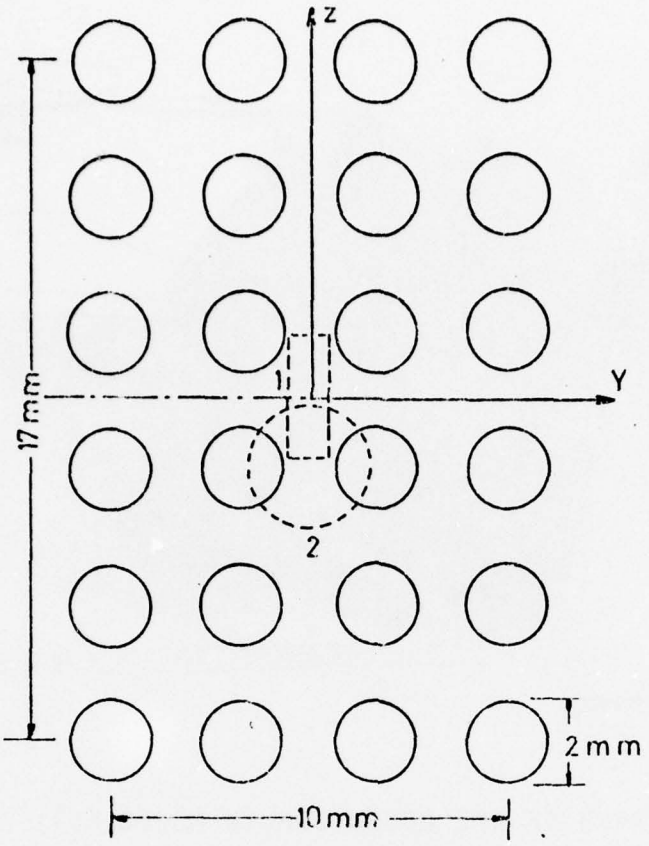

1. THIN FILM SURFACE TEMPERATURE SENSOR
   3mm x 1mm
2. COPPER CALORIMETER SENSOR
   3mm D.

FIG. 5 GEOMETRY OF ARRAY OF HOLES USED IN IMPINGEMENT HEAT TRANSFER CALIBRATOR

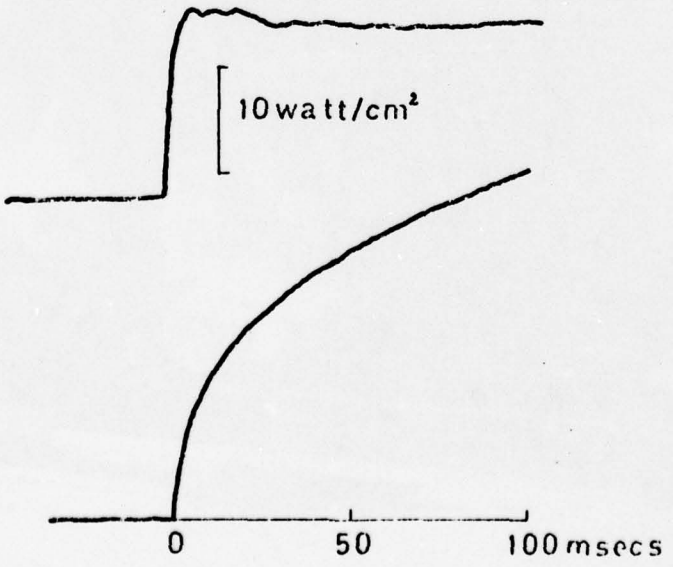

FIG. 6 TYPICAL SURFACE TEMPERATURE AND HEAT TRANSFER TRACES FROM THIN FILM SENSOR SUBJECTED TO CT1 CALIBRATOR

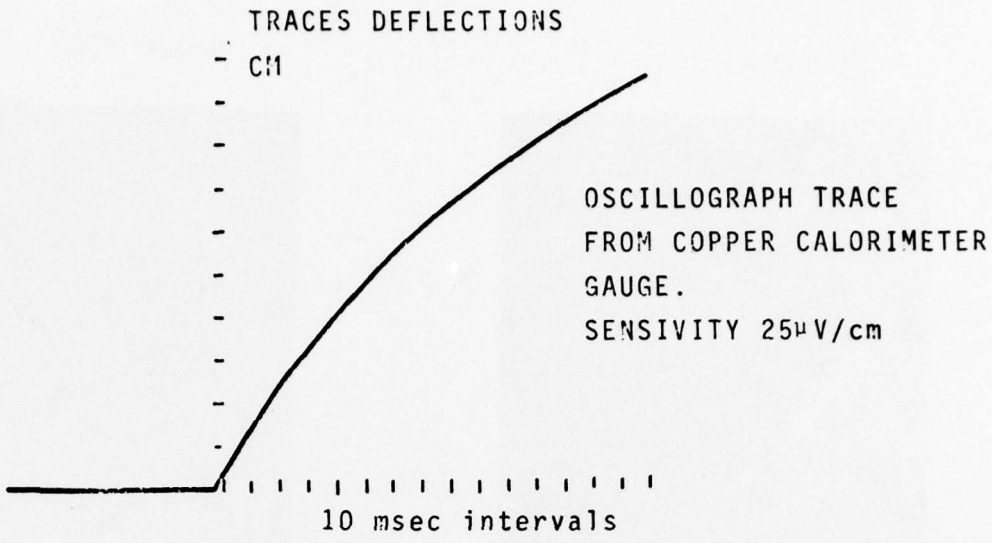

FIG. 7 TYPICAL TEMPERATURE TRACE FROM COPPER CALORIMETER SUBJECTED TO CT1 CALIBRATOR

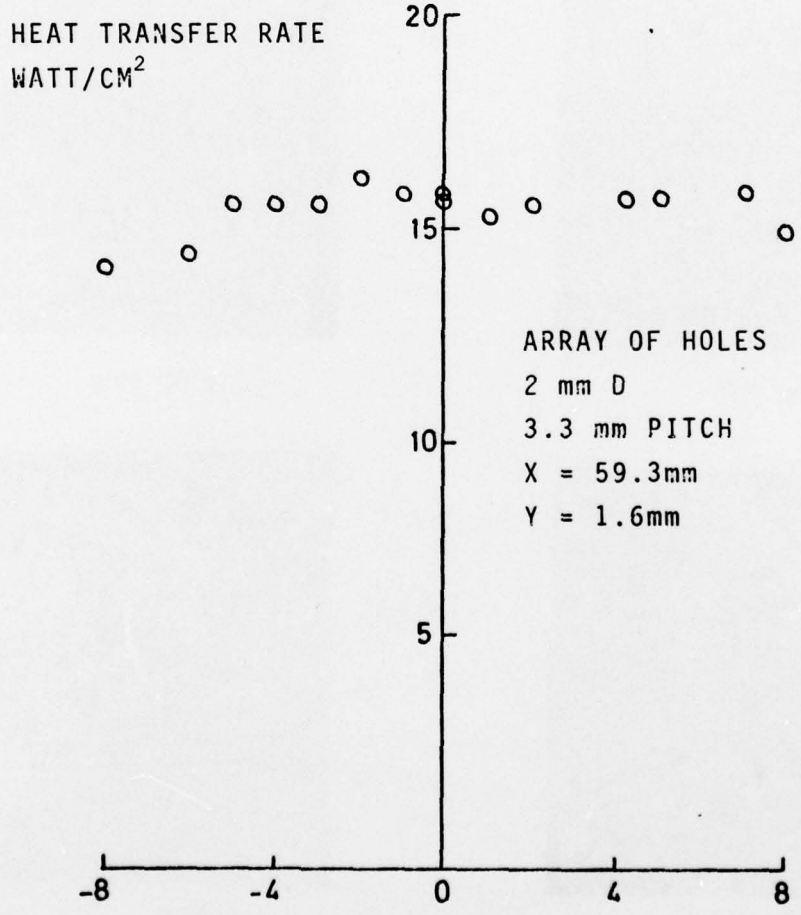

FIG. 8 HEAT TRANSFER DISTRIBUTION ACROSS AN ARRAY OF JETS EMANATING FROM HOLE GEOMETRY GIVEN IN FIG.5

MODEL K

MODEL K(R)

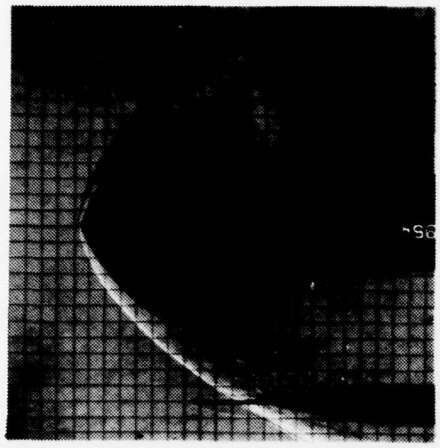

α = -3

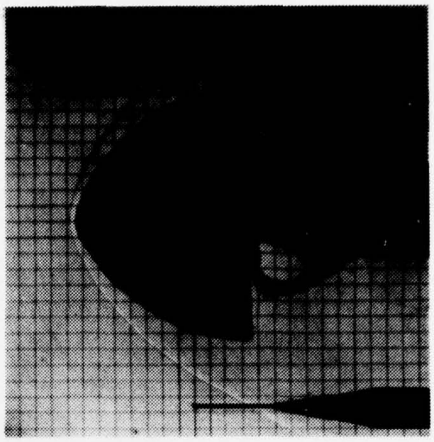

i)RUN 573

ii)RUN 582

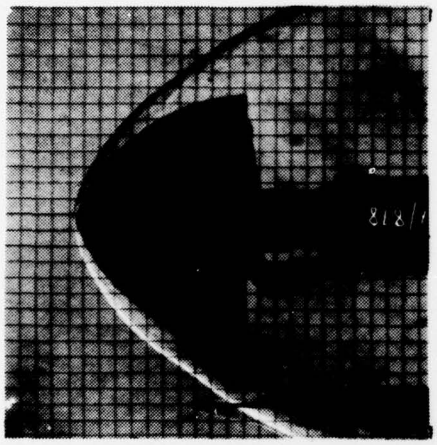

α = 0

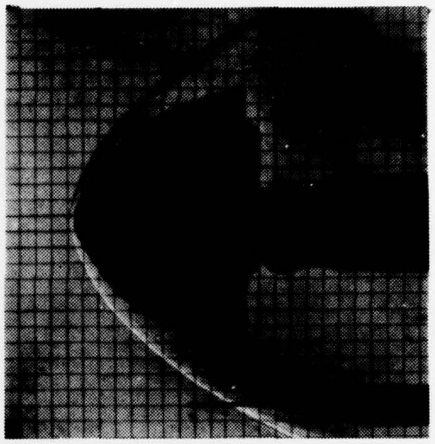

iii)RUN 566

iv)RUN 575

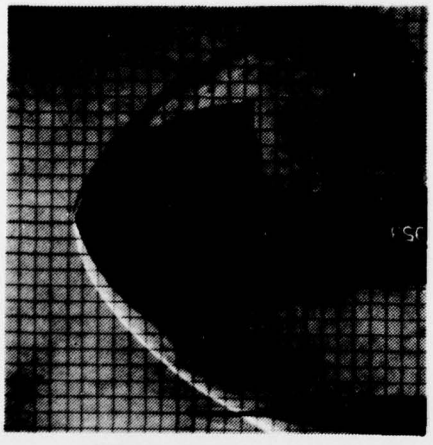

α = +3

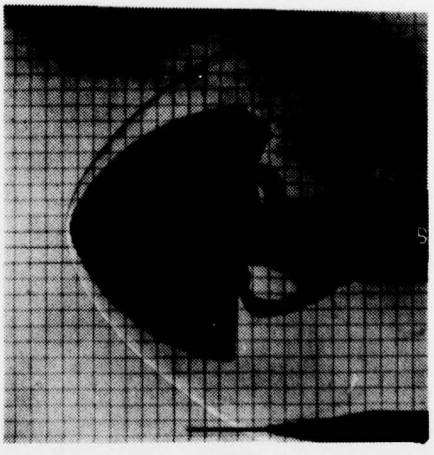

v)RUN 572

vi)RUN 583

FIG. 9a SCHLIEREN PHOTOGRAPHS M = 16, Re = 9 x 10^6

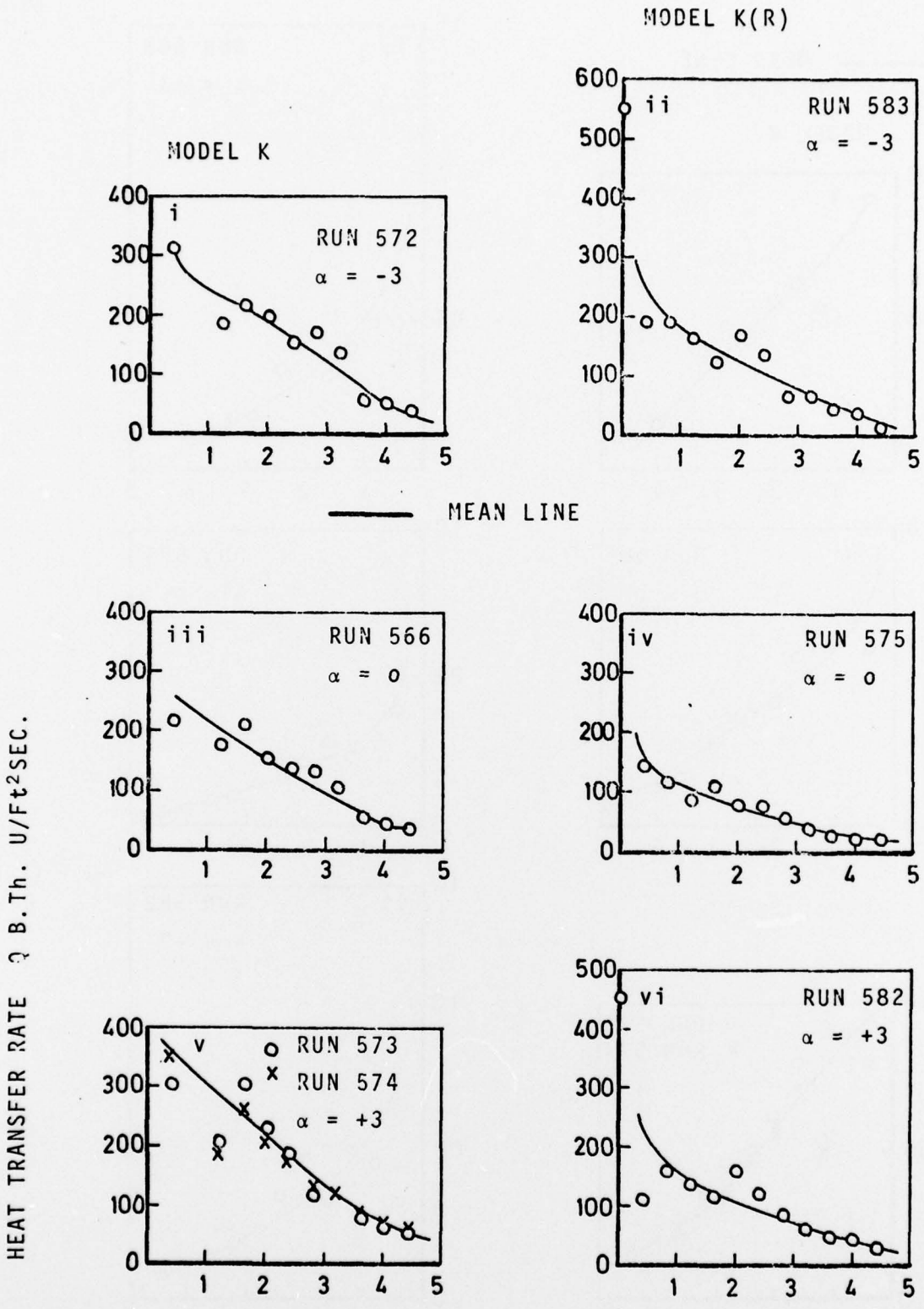

FIG. 9b. HEAT TRANSFER RATE MEASUREMENTS
M = 16, Re = 9 x 10^6 /ft.

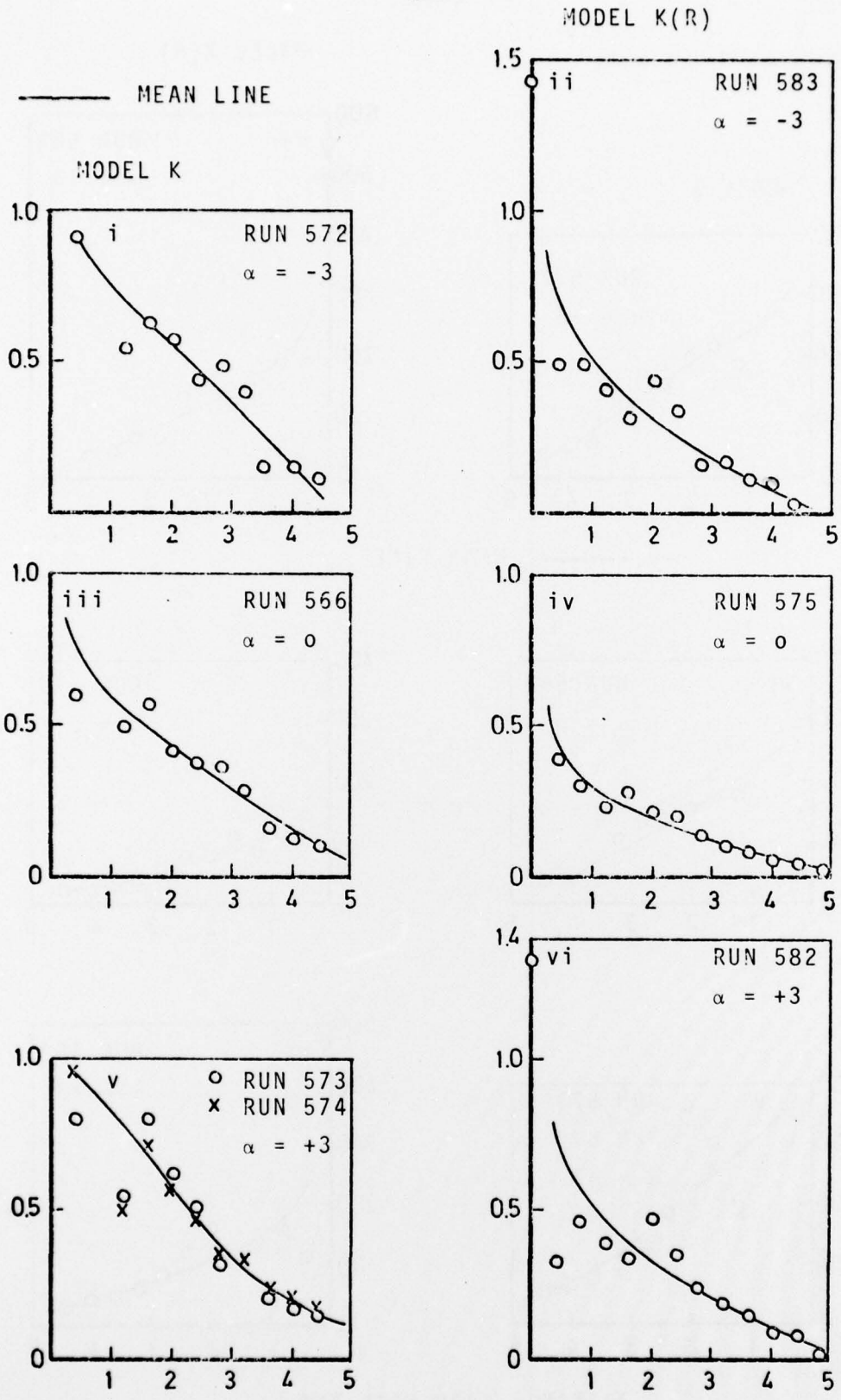

FIG. 9c NORMALIZED HEAT TRANSFER RATE
M = 16, Re = 9 x 10^6/ft.

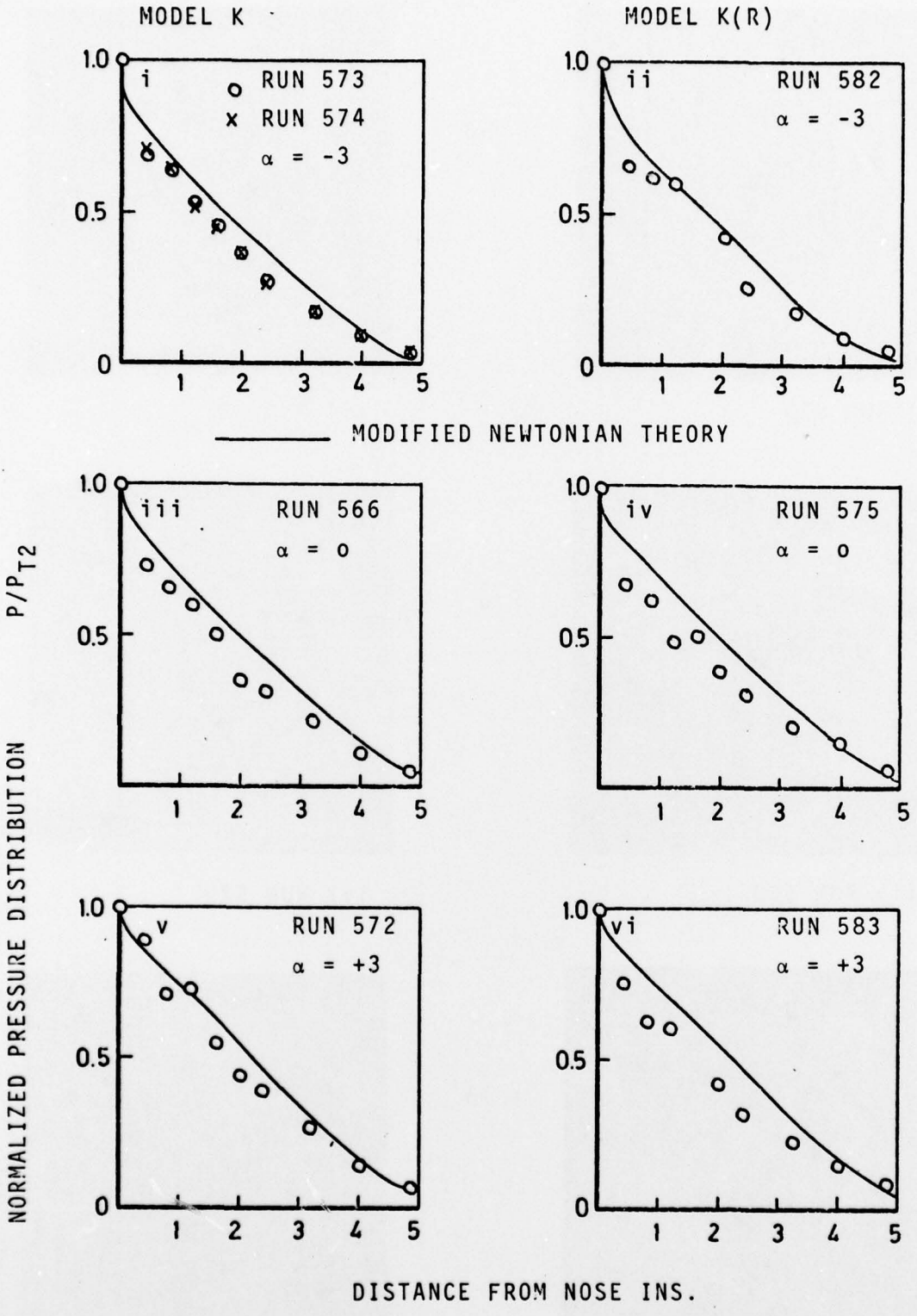

FIG. 9d NORMALIZED PRESSURE DISTRIBUTION.
M = 16, Re = 9 x 10^6 /ft

MODEL K

MODEL K(R)

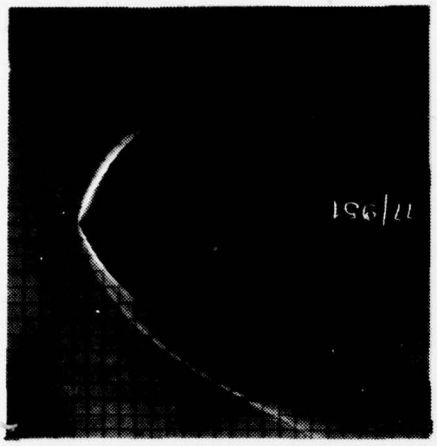

= -3

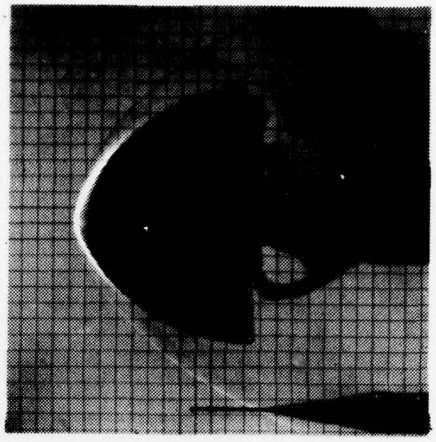

i) RUN 570

ii) RUN 581

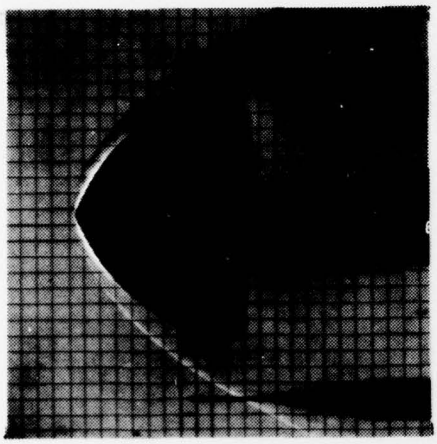

= o

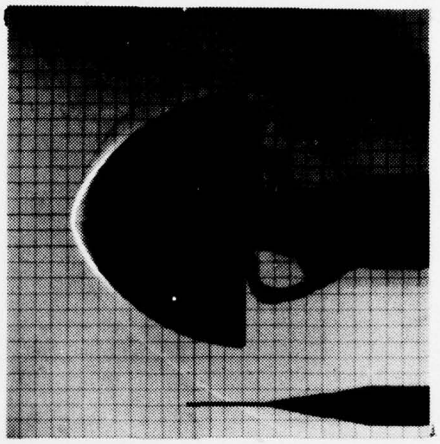

iii) RUN 568

iv) RUN 579

= +3

v) RUN 571

vi) RUN 580

FIG. 10a SCHLIEREN PHOTOGRAPHS M = 20, Re = 3 x 10^6/ft

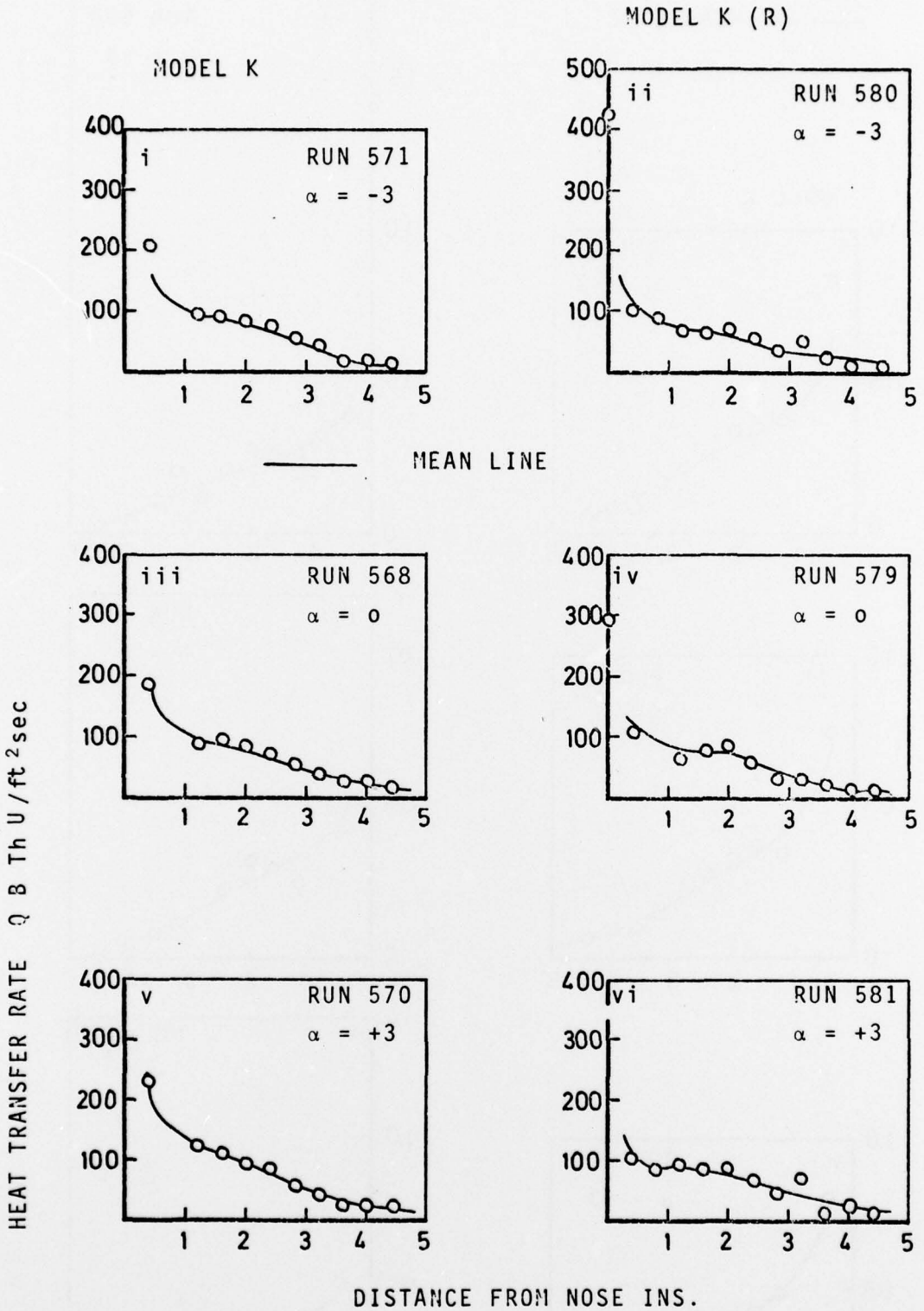

FIG. 10b HEAT TRANSFER MEASUREMENTS
M = 19, Re = 3 x 10^6/ft.

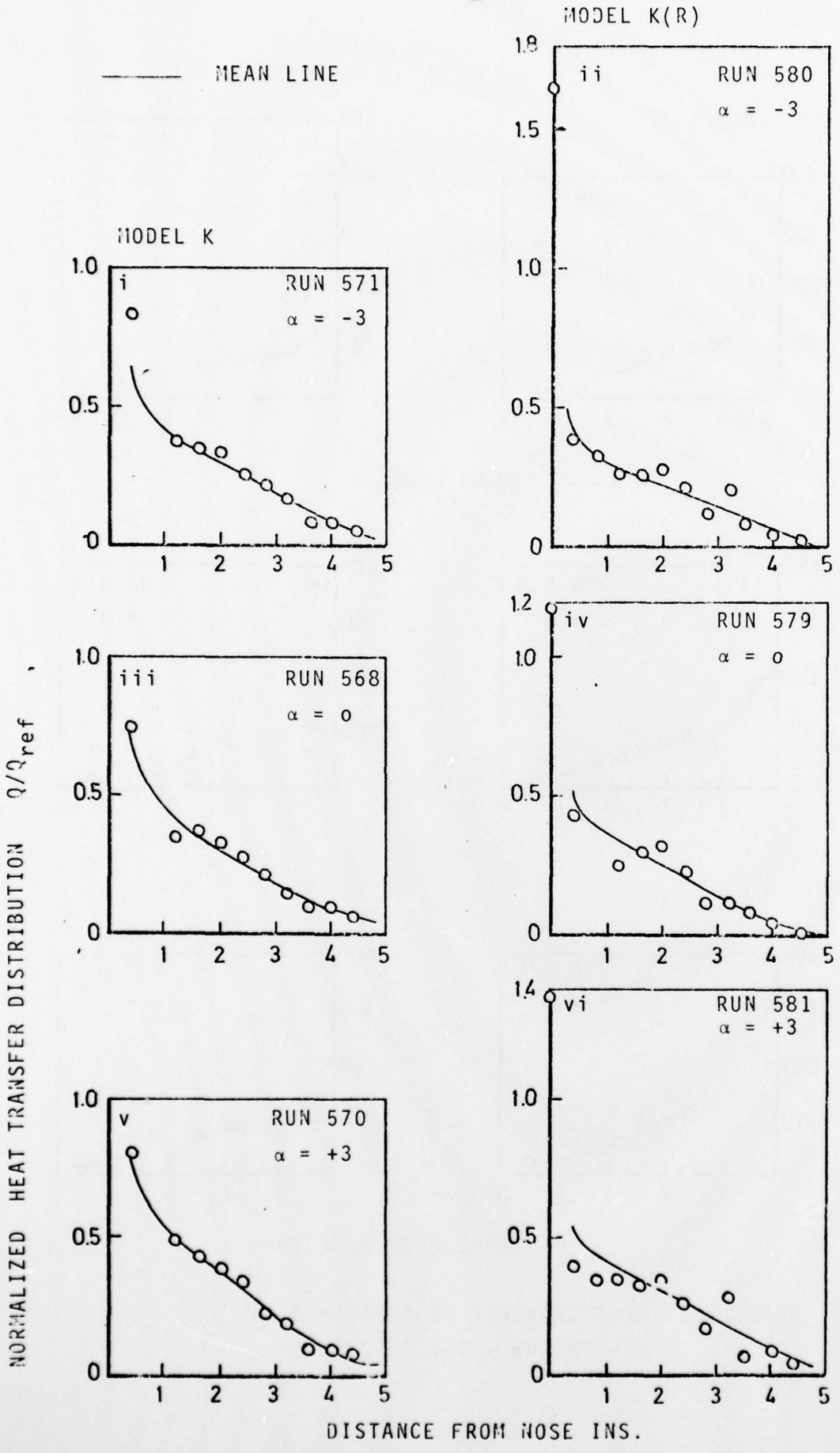

FIG. 10c NORMALIZED HEAT TRANSFER
M = 19, Re = 3 x 10^6/ft

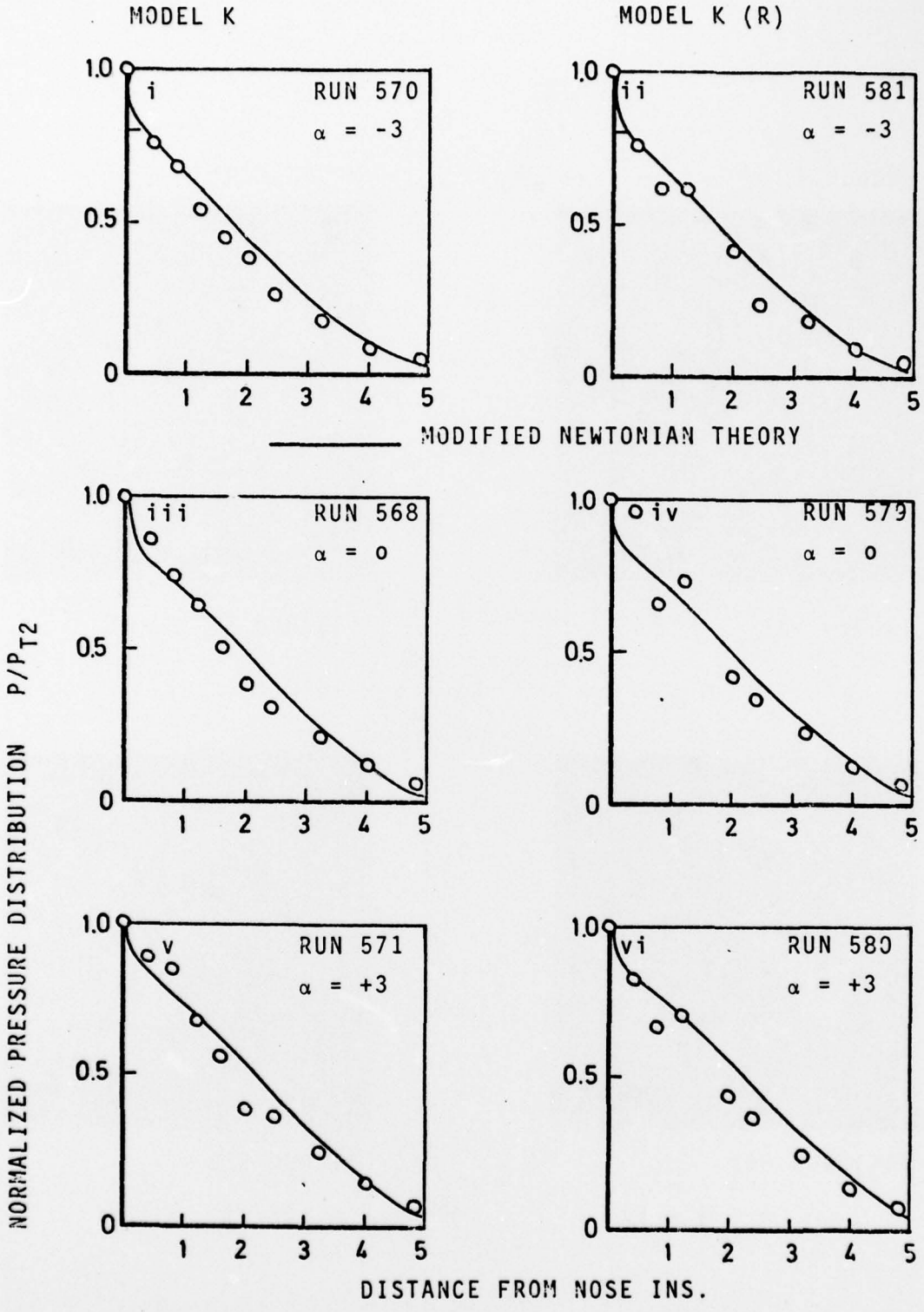

FIG. 10d NORMALIZED PRESSURE DISTRIBUTION
M = 19, Re = 3 x 10^6/ft.

MODEL K

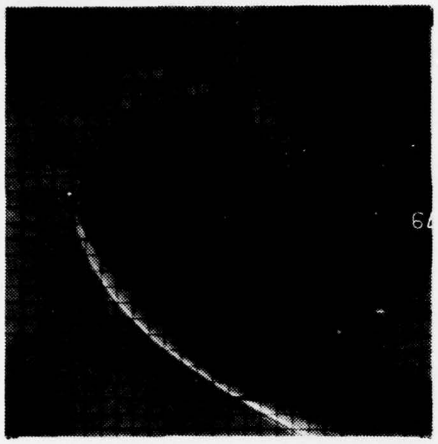

i) RUN 567

MODEL K(R)

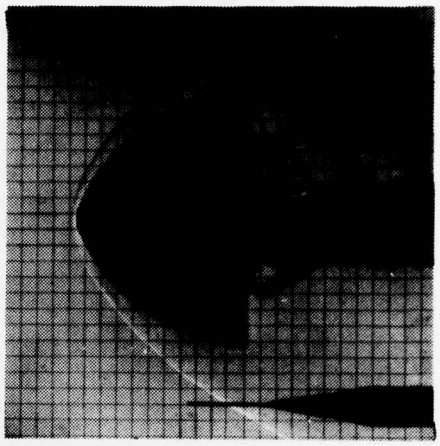

ii) RUN 577

M = 15 Re = 5 x 10^6/ft.

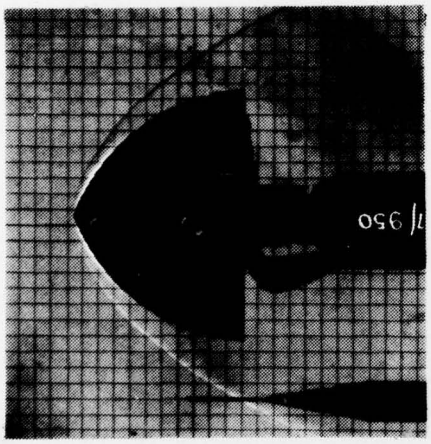

iii) RUN 569

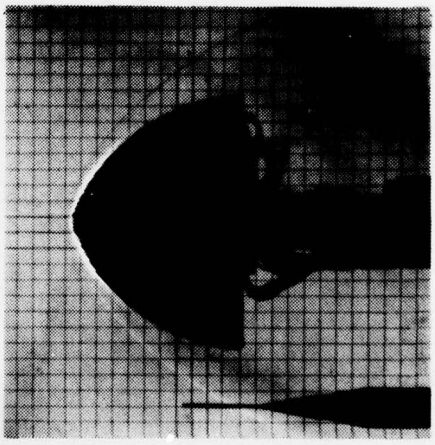

iv)RUN 578

M = 19 Re = 2 x 10^6/ft.

FIG. 11a SCHIEREN PHOTOGRAPHS.ZERO INCIDENCE.

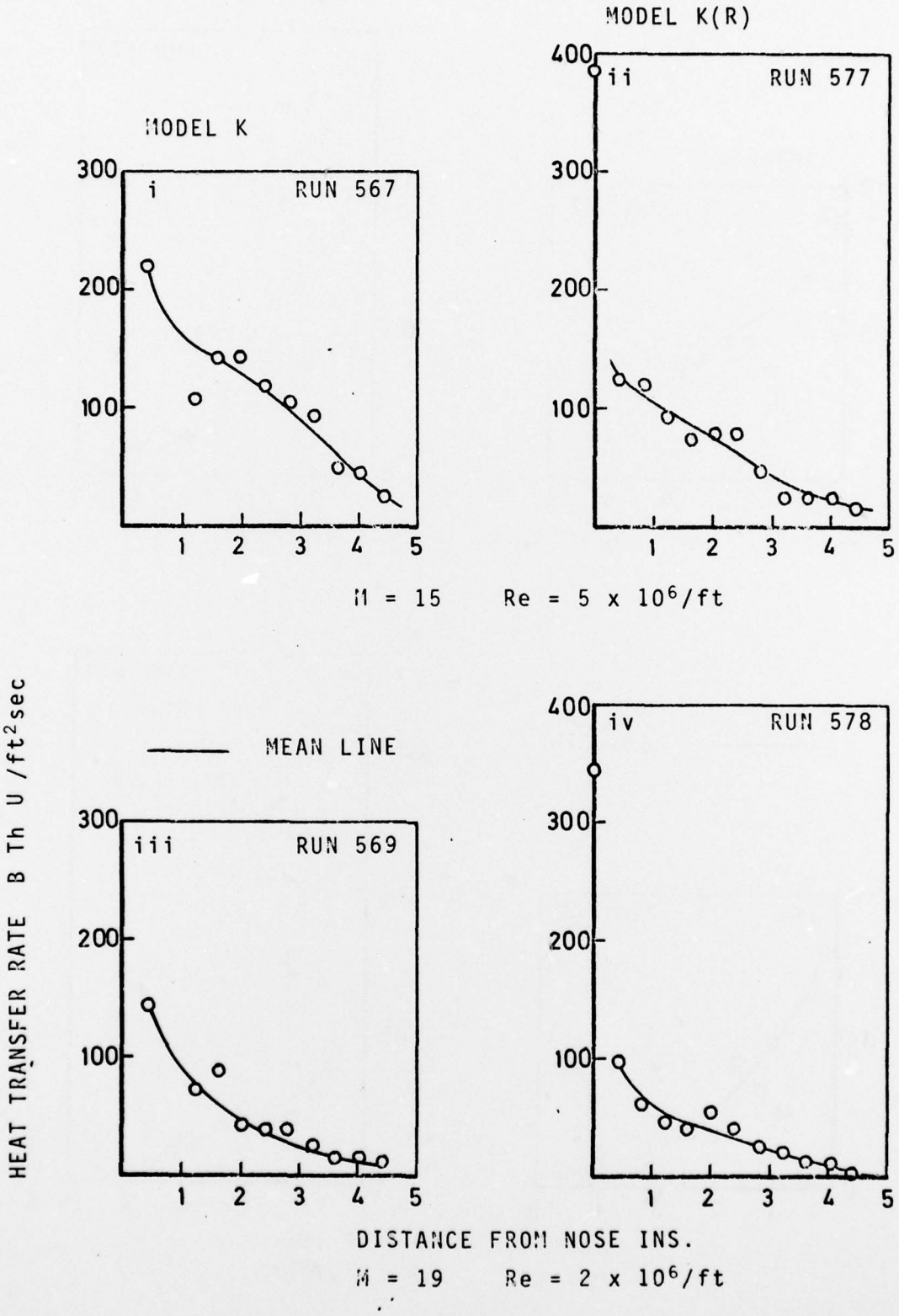

M = 15 Re = 5 x 10^6/ft

M = 19 Re = 2 x 10^6/ft

FIG. 11b HEAT TRANSFER DISTRIBUTION .ZERO INCIDENCE.

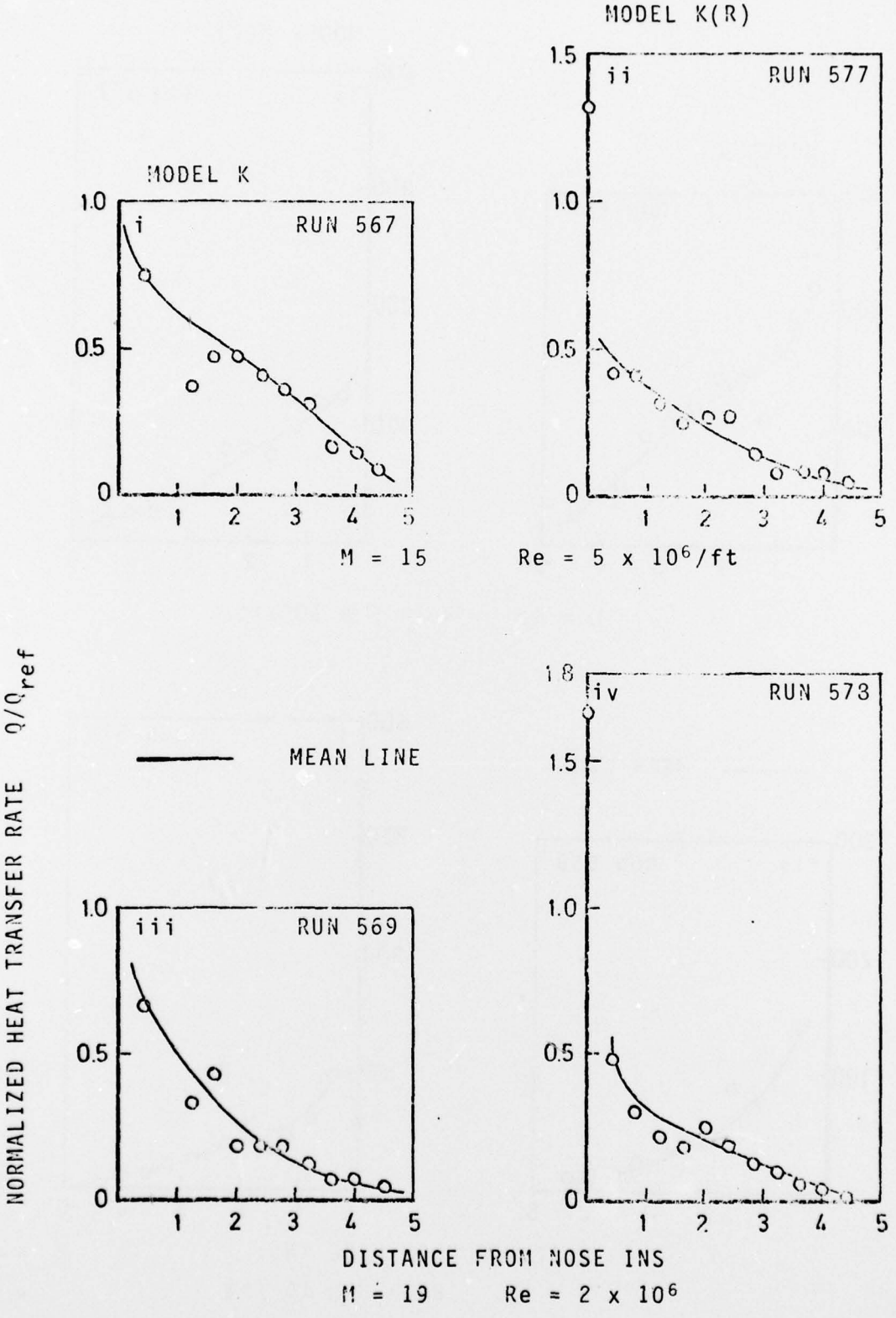

FIG. 11c NORMALIZED HEAT TRANSFER . ZERO INCIDENCE.

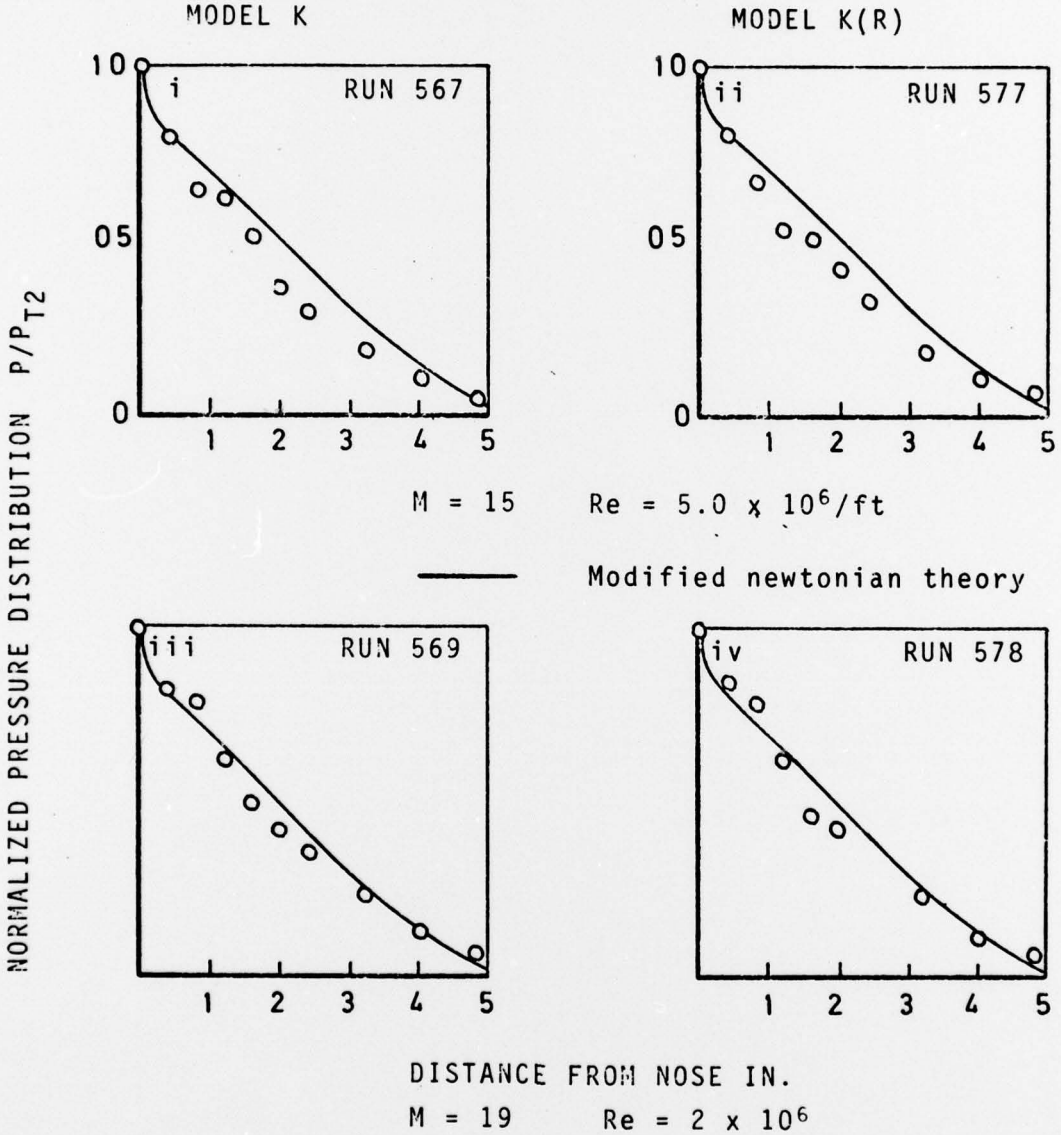

FIG. 11d NORMALIZED PRESSURE DISTRIBUTION
ZERO INCIDENCE.

SECURITY CLASSIFICATION OF THIS PAGE (When Data Entered)

REPORT DOCUMENTATION PAGE

READ INSTRUCTIONS BEFORE COMPLETING FORM

1. REPORT NUMBER: AFOSR-TR-78-0854	2. GOVT ACCESSION NO.
3. RECIPIENT'S CATALOG NUMBER	
4. TITLE (and Subtitle): EXPERIMENTAL STUDY OF THE HYPERSONIC FLOW OVER CONVEX CONIC MODEL RESEMBLING THE NOSETIP OF A REENTRY VEHICLE	5. TYPE OF REPORT & PERIOD COVERED: FINAL rept., 30 Nov 76 - 1 Dec 77
6. PERFORMING ORG. REPORT NUMBER: VKI-IN-59	
7. AUTHOR(s): BRYAN E. RICHARDS	8. CONTRACT OR GRANT NUMBER(s): AFOSR-76-2942
9. PERFORMING ORGANIZATION NAME AND ADDRESS: VON KARMAN INSTITUTE FOR FLUID DYNAMICS, CHAUSSÉE DE WATERLOO, 72, B-1640 RHODE SAINT GENÈSE, BELGIUM	10. PROGRAM ELEMENT, PROJECT, TASK AREA & WORK UNIT NUMBERS: 2307A1, 61102F
11. CONTROLLING OFFICE NAME AND ADDRESS: AIR FORCE OFFICE OF SCIENTIFIC RESEARCH/NA, BLDG 410, BOLLING AIR FORCE BASE, D C 20332	12. REPORT DATE: 11 1978
	13. NUMBER OF PAGES: 43 (12 46p.)
14. MONITORING AGENCY NAME & ADDRESS (if different from Controlling Office)	15. SECURITY CLASS. (of this report): UNCLASSIFIED
	15a. DECLASSIFICATION/DOWNGRADING SCHEDULE

16. DISTRIBUTION STATEMENT (of this Report)

Approved for public release; distribution unlimited.

17. DISTRIBUTION STATEMENT (of the abstract entered in Block 20, if different from Report)

16 2307 17 A1

18. SUPPLEMENTARY NOTES

19. KEY WORDS (Continue on reverse side if necessary and identify by block number)

HYPERSONIC FLOW
REENTRY
ABLATION
HEAT TRANSFER MEASUREMENTS
PRESSURE MEASUREMENTS

20. ABSTRACT (Continue on reverse side if necessary and identify by block number)

Heat transfer and pressure measurements have been measured on a convex conic configuration with a spherical nosetip in the von Karman Institute Longshot free piston tunnel at M=15 and 20. The test flow parameters achieved closely simulated reentry aerodynamic conditions. Information derived from the measurements and also from schlieren photographs enabled statements to be made on the effect of Mach number, Re number, surface roughness and flow incidence on the flow over the model.

DD FORM 1 JAN 73 1473 EDITION OF 1 NOV 65 IS OBSOLETE

UNCLASSIFIED

SECURITY CLASSIFICATION OF THIS PAGE (When Data Entered)

367 475